SINGLE EVENT KINETIC MODELING OF THE HYDROCRACKING OF PARAFFINS

A Thesis

by

HANS KUMAR

Submitted to the Office of Graduate Studies of
Texas A&M University
in partial fulfillment of the requirements for the degree of

MASTER OF SCIENCE

August 2004

Major Subject: Chemical Engineering

SINGLE EVENT KINETIC MODELING OF THE HYDROCRACKING OF PARAFFINS

A Thesis

by

HANS KUMAR

Submitted to Texas A&M University
in partial fulfillment of the requirements
for the degree of

MASTER OF SCIENCE

Approved as to style and content by:

Gilbert F. Froment
(Chair of Committee)

Rayford G. Anthony
(Member)

D. Wayne Goodman
(Member)

Kenneth R. Hall
(Head of Department)

August 2004

Major Subject: Chemical Engineering

ABSTRACT

Single Event Kinetic Modeling of the Hydrocracking

of Paraffins. (August 2004)

Hans Kumar, B.E., University of Roorkee, India

Chair of Advisory Committee: Dr. Gilbert F. Froment

A mechanistic kinetic model for the hydrocracking of paraffins based on the single-event kinetics approach has been studied. Several elements of the model have been improved and the parameters of the model have been estimated from experimental data on n-hexadecane hydrocracking.

A detailed reaction network of elementary steps has been generated based on the carbenium ion chemistry using the Boolean relation matrices. A total of 49,636 elementary steps are involved in the hydrocracking of n-hexadecane. The rate coefficients of these elementary steps are expressed in terms of a limited number of single event rate coefficients. By virtue of the single event concept, the single event rate coefficients of a given type of elementary steps are independent of the structure of reactant and product. Given their fundamental nature they are also independent of the feedstock composition and the reactor configuration. There is no lumping of components involved in the generation of the reaction network. Partial lumping is introduced only at a later stage of the model development and the lumping is strictly based on the criterion that the individual components in any lump will be in thermodynamic equilibrium. This definition of lumping requires a total of 49 pure components/lumps in the kinetic model for the hydrocracking of n-hexadecane. The “global” rate of reaction of a lump to another lump is expressed using lumping coefficients which account for the transformation of all the components of one lump into the components of another lump

through to a given type of elementary steps. The rate expressions thus formulated are inserted into a one-dimensional, three-phase plug flow reactor model. Experimental data have been collected for the hydrocracking of n-hexadecane. The model parameters are estimated by constrained optimization using sequential quadratic programming by minimizing the sum of squares of residuals between experimental and model predicted product profiles. The optimized parameters are finally used for the reactor simulation to study the effect of different process variables on the conversion and product distribution of n-hexadecane hydrocracking. The model is also used to predict the product distribution for the hydrocracking of a heavy paraffinic mixture consisting of C_9 to C_{33} normal paraffins.

ACKNOWLEDGMENTS

I would like to express my sincere gratitude to Prof. Gilbert F. Froment for his guidance and assistance in this project. The technical discussions with Prof. Froment had always been very insightful and I would always be indebted to him for all the knowledge he shared with me. His prompt responses to all my email queries are truly appreciated.

I would like to thank my committee members: Prof. Rayford G. Anthony and Prof. D. Wayne Goodman. The reality is that Prof. Anthony was much more than a committee member for me. He always helped me in all the technical and non-technical issues during this work. His encouragement and efforts led this project to be completed successfully in a timely fashion. I would also like to thank Prof. Jack H. Lunsford for all his time and efforts and the new ideas he gave me during the discussions with him.

My special thanks go to Dr. J. Govindhakannan. I had a wonderful time with him discussing different aspect of research and life. This project would not have been completed without his past research work in this field. His contribution in this field is highly appreciated.

Many thanks to my friends and my group members for making my research at Texas A&M University a pleasant and exciting experience. Arnab, Amit, Faisal, Srini, Abhay, Nitin, Greg, Sumit, Sanjay, Nishant, Vipin, Mert, Hemendra, thanks a lot!

Finally, I would like to express my warmest thanks to my parents and family members for their love.

TABLE OF CONTENTS

Page

ABSTRACT iii

ACKNOWLEDGMENTS v

TABLE OF CONTENTS vi

LIST OF TABLES viii

LIST OF FIGURES ix

CHAPTER I INTRODUCTION 1

1.1 Importance of Hydrocracking Process 1
1.2 Process Description 2
1.3 Brief Literature Review 5

CHAPTER II CHEMISTRY AND MECHANISM OF HYDROCRACKING REACTIONS 7

2.1 Chemistry of the Hydrocracking Reactions 7
2.2 Mechanism of Acid Catalyzed Steps 12
2.2.1 Isomerization Steps 12
2.2.2 Cracking Steps 13

CHAPTER III SINGLE EVENT KINETICS AND REACTION NETWORK GENERATION 16

3.1 Theory of Single-Event Kinetics 16
3.2 Generation of the Reaction Network 18
3.2.1 Representation of Chemical Species 19
3.2.2 Standardization of Labeling 21
3.2.3 Generation of Elementary Steps 21
3.3 Rules for Generating the Reaction Network 24
3.4 Reaction Network for n-Hexadecane 25

CHAPTER IV MODEL PARAMETERS AND DEVELOPMENT OF RATE EXPRESSIONS 27

4.1 Kinetic Parameters in the Model 27
4.1.1 Isomerization Steps 28

Page

4.1.2 Cracking Steps 29
4.1.3 Protonation / Deprotonation Steps 30
4.1.4 Thermodynamic Constraints 33
4.1.5 Hydrogenation/Dehydrogenation 34
4.1.6 Parameters for Physical Adsorption 34
4.2 Summary of Model Parameters 36
4.3 Development of Rate Expressions 37

CHAPTER V PARAMETER ESTIMATION AND REACTOR SIMULATION RESULTS 45

5.1 Reactor Model and Parameter Estimation 45
5.2 Sensitivity Study of Parameters 48
5.3 Temperature Dependency of the Parameters 51
5.4 Reactor Simulation Results and Discussion 55
5.4.1 Effect of Temperature 55
5.4.2 Effect of Total Pressure 56
5.4.3 Effect of Hydrogen to Hydrocarbon Ratio 58
5.4.4 Reactor Simulation for a Different Feed 58

CHAPTER VI SUMMARY AND CONCLUSIONS 71

NOMENCLATURE 72

REFERENCES 74

VITA 76

LIST OF TABLES

TABLE Page

3.1 Results of Network Generation for C_{16} and C_{33} Feedstocks 26

4.1 List of Model Parameters 37

5.1 Parameters Estimated from Experimental Data 48

5.2 Feed and Product Composition for the Heavy Paraffinic Mixture 60

LIST OF FIGURES

FIGURE Page

1.1 Simplified process flow diagram of a two stage hydrocracker 4

2.1 Zeolite structures for (a) Mordenite (b) Faujasite 8

2.2 Schematic representation of the reaction scheme of hydrocarbon molecule at the catalyst surface 9

2.3 List of elementary steps for the hydrocracking of paraffins 10

2.4 Schematic representation of various physical and chemical phenomena taking place in hydrocracking of paraffins 11

2.5 Mechanism of methyl shift steps 12

2.6 Mechanism of PCP steps 12

2.7 Type of β-scission steps 14

3.1 Boolean relation representation of 2-methyl-5-hexyl and characterization vector 20

3.2 2-methyl-4-hexyl and its characterization vector 22

3.3 β positions of 2-methyl-5-hexyl carbenium ion 23

3.4 Algorithm for the network generation for paraffins 24

4.1 Reaction pathway between two olefins through a carbenium ion 30

4.2 Reaction pathway between two carbenium ions through an olefin 33

4.3 Reaction scheme between the lumps/components per carbon number 43

5.1 Structure of reactant giving a t-carbenium ion and an iso-olefin on cracking 50

5.2 Temperature dependency of parameters
1-$\tilde{k}^{*}_{PCP}(s;s)$, 4-$\tilde{k}^{*}_{Cr}(s;s,no)$, 5-$\tilde{k}^{*}_{Cr}(s;s,io)$, 6-$\tilde{k}^{*}_{Cr}(s;t,no)$, 7-$\tilde{k}^{*}_{Cr}(s;t,io)$ 53

FIGURE Page

5.3 Temperature dependency of parameters
$2\text{-}\tilde{k}^{*}_{PCP}(s;t)$, $3\text{-}\tilde{k}^{*}_{PCP}(t;t)$ ……..53

5.4 Temperature dependency of parameters
$8\text{-}\tilde{k}^{*}_{Cr}(t;s,io)$, $9\text{-}\tilde{k}^{*}_{Cr}(t;t,io)$ 54

5.5 Temperature dependency of parameters
$10\text{-}K_{L,np}$, $11\text{-}K_{L,mbp}$, $12\text{-}K_{L,dbp}$, $13\text{-}K_{L,tbp}$ ……...54

5.6 Conversion of hexadecane with space time
(P = 35.5 bars, T = 304.4 ^{o}C & γ = 9.0) 61

5.7 Molar distribution of products based on degree of branching
(P = 35.5 bars, T = 304.4 ^{o}C & γ = 9.0) 61

5.8 Selectivities of products based on carbon number at different cracking conversions (P = 35.5 bars, T = 304.4 ^{o}C & γ = 9.0) 62

5.9 Total moles of cracked products formed per 100 moles of hexadecane cracked at different cracking conversions
(P = 35.5 bars, T = 304.4 ^{o}C & γ = 9.0) 62

5.10 Conversion of hexadecane with space time
(P = 35.5 bars, T = 321.3 ^{o}C & γ = 9.0) 63

5.11 Molar distribution of products based on degree of branching
(P = 35.5 bars, T = 321.3 ^{o}C & γ = 9.0) 63

5.12 Selectivities of products based on carbon number at different cracking conversions (P = 35.5 bars, T = 321.3 ^{o}C & γ = 9.0) 64

5.13 Total moles of cracked products formed per 100 moles of hexadecane cracked at different cracking conversions
(P = 35.5 bars, T = 321.3 ^{o}C & γ = 9.0) 64

5.14 Conversion of hexadecane with space time
(P = 35.5 bars, T = 332.4 ^{o}C & γ = 9.0) 65

5.15 Molar distribution of products based on degree of branching
(P = 35.5 bars, T = 332.4 ^{o}C & γ = 9.0) 65

FIGURE Page

5.16 Selectivities of products based on carbon number at different cracking conversions (P = 35.5 bars, T = 332.4 ^{o}C & γ= 9.0) 66

5.17 Total moles of cracked products formed per 100 moles of hexadecane cracked at different cracking conversions (P = 35.5 bars, T = 332.4 ^{o}C & γ = 9.0) 66

5.18 Isomerization conversion vs. total conversion at different temperatures (P = 35.5 bars & γ = 9.0) 67

5.19 Selectivities of products based on carbon number at different temperatures and same cracking conversion (P = 35.5 bars & γ = 9.0) 67

5.20 Effect of total pressure at the hexadecane conversion (T = 304.4 ^{o}C, γ = 9.0) 68

5.21 Effect of hydrogen to hydrocarbon ratio on conversion (T = 304.4 ^{o}C, P = 35.5 bar, space time = 500.0 kg cat. h/kmol) 68

5.22 Concentration profile of hydrogen in gas phase along the bed length at different values of H_2 to HC ratio R (T = 304.4 ^{o}C, P = 35.5 bar) 69

5.23 Concentration profile of hydrogen in liquid phase along the bed length at different values of H_2 to HC ratio R (T = 304.4 ^{o}C, P = 35.5 bar) 69

5.24 Product distribution per carbon number for the heavy paraffinic feed (T = 321.3 ^{o}C, P = 35.5 bar, γ = 35.5, LHSV = 1.0 hr^{-1}) 70

5.25 Product profiles along the bed length for the heavy paraffinic feed (T = 321.3 ^{o}C, P = 35.5 bar, γ = 35.5, LHSV = 1.0 hr^{-1}) 70

CHAPTER I

INTRODUCTION

1.1 Importance of Hydrocracking Process

Hydrocracking is a catalytic petroleum refining process that converts heavy, high boiling feedstock molecules to smaller, lower boiling ones through carbon-carbon bond breaking preceded by isomerization and accompanied by simultaneous or sequential hydrogenation. Hydrocracking is a process of considerable flexibility because it allows the conversion of a wide range of feedstocks to a variety of desired products.[1]

Catalytic hydrocracking has become a major operation in today's oil refining industry to produce middle distillates with excellent product qualities. In addition to the hydrocracking of VGO and other refinery residues, the hydrocracking of Fischer-Tropsch wax has recently been recognized as one of the promising processes to produce middle distillate of very high quality.[2] The synthetic diesel produced by this process has a cetane number of more than 74 with zero sulfur content.[3,4]

Developing reliable kinetic models for the hydrocracking process is an important activity from a commercial as well as a research viewpoint.[5] The design and optimization of the hydrocracking units require a detailed kinetic model that can take into account the complexity of the feedstock while following the rules of the underlying carbenium ion chemistry.[6] The use of comprehensive process models with an accurate representation of hydrocracking kinetics at the elementary step level can be used to reduce expensive experimentation in pilot plants.

This thesis follows the style and format of the *Journal of Physical Chemistry B*.

These mathematical models can also be used successfully in process design to predict the detailed product distribution and optimum operating conditions for a range of feedstocks and, in addition, for a more efficient selection of catalysts.

1.2 Process Description

Many different flow schemes have been developed for the hydrocracking process so that various feedstocks can be processed to produce a full range of products. All of the processes are vendor specific with respect to the reactor design and catalyst selection. The three major schemes for hydrocracking processes can be classified as follows:

1) Single-stage recycle hydrocracking
2) Two-stage recycle hydrocracking
3) Once through hydrocracking

In general, the commercial hydrocracking plants are operated at the following conditions:[1]

Catalyst bed temperature	300-450^{o} C
Pressure	85-200 bars
Liquid hourly space velocity	0.5-2.5 hr^{-1}
H_2/HC ratio	3,000-10,000 SCFB
H_2 consumption	1,200-3,500 SCFB

Due to high hydrogen partial pressures and the use of dual function catalysts, the rate of catalyst coking and deactivation is very low, resulting in on-stream cycle lengths of several years.

The typical feedstocks used in hydrocracking process contain sulfur, nitrogen, and in case of resid feedstock, metals such as nickel and vanadium. Because such compounds

have a deleterious effect on hydrocracking catalyst, the feedstock typically requires hydrotreatment prior to contact with the hydrocracking catalyst. For this reason, most of the hydrocracking processes are two stage involving both hydrotreatment and hydrocracking.

Figure 1.1 shows the simplified flow diagram for a two stage hydrocracking process with recycle. The vacuum gas oil is sent to the first stage of the hydrocracker and is severely hydrotreated. Most of the sulfur and nitrogen compounds are removed from the oil and many of the aromatics are saturated. In addition, significant conversion to light products occurs in the first stage. The liquid products from the first stage are sent to a common fractionation section. To prevent overcracking, lighter products are removed by distillation. The unconverted oil from the bottom of the fractionator is routed to the second stage reactor section. The second reaction stage saturates almost all the aromatics and cracks the oil feed to light products. Due to the saturation of aromatics, the second stage produces excellent quality products. The liquid product from the second stage is sent to the common fractionator where light products are distilled. The second stage operates in a recycle to extinction mode with per-pass conversions ranging from 50 to 80%. The following products are obtained from fractionation: light ends (C_4^-), light naphtha (C_5 – 80 ^oC), heavy naphtha (80 ^oC – 150 ^oC), jet fuel/kerosene (150 ^oC – 290 ^oC), and diesel fuel (290 ^oC – 370 ^oC). The fractionator bottoms containing the unconverted feed (370 ^oC +) is recycled to the second stage reactor so that it can be converted into commercial products.

The overhead liquid and vapor from the hydrocracker fractionator is further processed in a light ends recovery unit where fuel gas, liquefied petroleum gas (LPG) and, naphtha are separated. The hydrogen supplied to the reactor sections of the hydrocracker comes from steam reformers. The hydrogen is compressed in stages until it reaches system pressure of the reactor sections.

The catalyst in the first reactor is designed to eliminate the hetero compounds in the feedstock and to convert the organic sulfur and nitrogen to hydrogen sulfide and ammonia, respectively. Such catalysts typically comprise sulfided molybdenum or tungsten and nickel or cobalt on an alumina support. The deleterious effect of H_2S and NH_3 on hydrocracking catalyst is considerably less than those of the corresponding organic hetero compounds. The hydrotreating catalyst also facilitates the hydrogenation of aromatics.

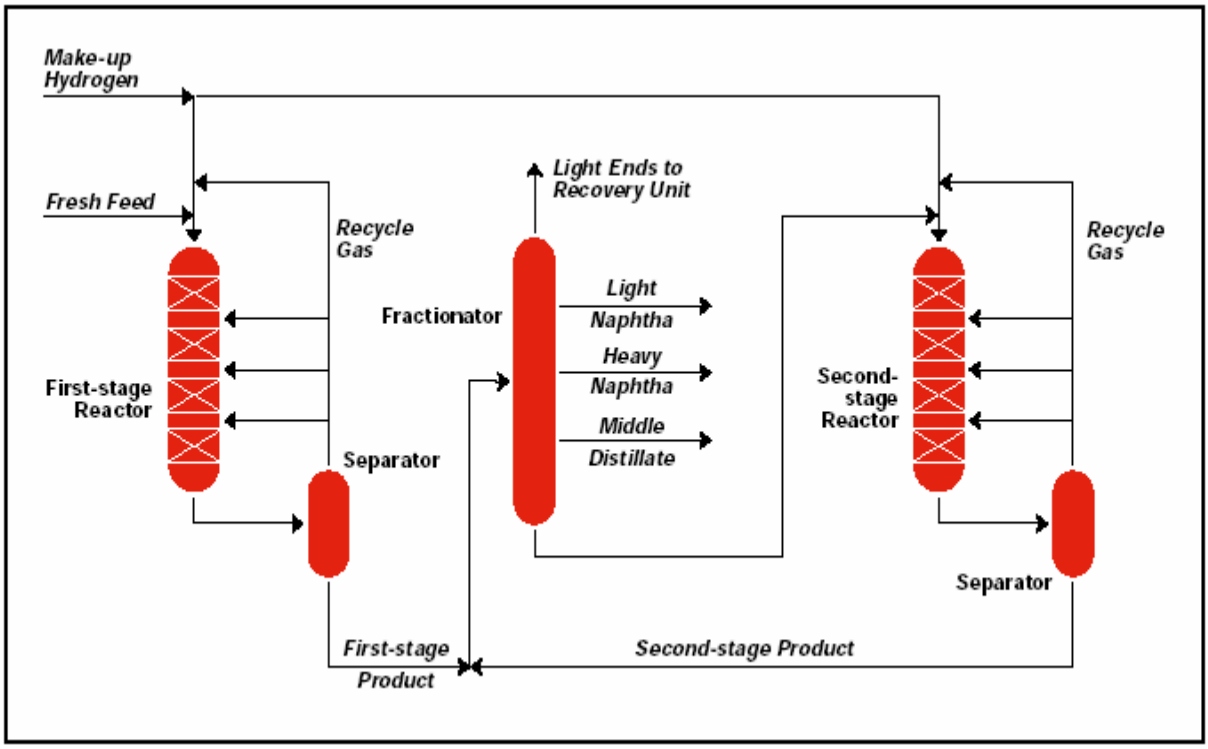

Figure 1.1 Simplified process flow diagram of a two stage hydrocracker

The hydrocracking catalyst in the second stage is designed to optimize the yields and quality of the desired products. Various reactions such as hydrogenation, dehydrogenation, isomerization, cracking, alkylation, dealkylation, etc. predominately take place in the second stage reactor. Hydrogenation reactions are highly exothermic whereas the cracking reactions are endothermic. The amount of heat liberated in the

hydrogenation reactions is greater than the heat required for the endothermic cracking reactions. The surplus heat released causes the reactor temperature to increase, thereby accelerating the reaction rate. Cold hydrogen is injected between the reactor beds as a quench to control the reactor temperature profile.[5]

The severity of the hydrocracking operation is measured by the degree of conversion of the feed to the lighter products. Conversion is defined as the volume percent of the feed, which disappears to form the products boiling below the desired product end point. A given percent conversion at a low product endpoint represents a more severe operation than does the same percent conversion at a higher product endpoint.

1.3 Brief Literature Review

To study the conversion of complex feedstocks, most efforts have focused on the development of lumped kinetic models in which the feedstock is divided into several lumps based on the boiling point range. A simplified reaction network between these lumps is set up and the rate coefficients for the global conversion of lumps are estimated from the experimental data. For example in the three lump model of Weekman and Nace,[7] the feedstock charge is converted to the gasoline boiling fraction and the remaining fraction by the following equations,

$$C_1 \xrightarrow{k_1} a_1 C_2 + a_2 C_3 \tag{1.1}$$

$$C_2 \xrightarrow{k_2} C_3 \tag{1.2}$$

In the above equations, C_1 represents the gas oil charged, C_2 represents the C_5-410 ^{o}F gasoline fraction and, C_3 represents the butanes, dry gas and, coke. The coefficients a_1 and a_2 represent the mass of C_2 and C_3 produced per mass of C_1 converted, respectively.

A more detailed lumped model was developed by Jacob et al.[8] with the introduction of 10 lumps. To achieve higher accuracy in the product yields predicted by the model, more and more lumps were introduced by various researchers. Increasing the number of lumps

also leads to the introduction of more parameters in the kinetic model. The major fundamental limitation of the lumped kinetic models is that the kinetic parameters depend on the feedstock as well as on the reactor configuration. Therefore, with every different feedstock the kinetic model needs to be refitted and new sets of parameters have to be estimated. This type of problem associated with the lumped models gave thrust to the development of mechanistic models.

The mechanistic models consider the carbenium ion chemistry of the elementary steps of isomerization and cracking. Quann and Jaffe[9] developed a kinetic model based on Structures Oriented Lumping (SOL). Their lumping strategy is based on molecular structure of the feed and products, and this approach is very close to the chemistry of the hydrocracking process.

Froment and co-workers[10,11] developed a mechanistic kinetic model starting from the elementary steps of the carbenium ion chemistry, and based on their concept it was named as single event kinetic model. Baltanas et al.[10] generated a complete network of elementary steps involving carbenium ions using a computer algorithm based on the approach devised by Clymans et al.[12] Vynckier et al.[11] extended the single event approach to complex feedstocks by introducing partial lumping and lumping coefficients. The lumping coefficients account for the contribution of every individual elementary step between the components of two lumps and the rate expressions written in term of lumping coefficients provide the global rate of transformation of one lump to another. Feng et al.[13] applied the single event approach to the catalytic cracking of paraffins on a RE-Y zeolite catalyst. Svoboda et al.[14] determined the single event rate parameters for the hydrocracking of n-octane. Martens et al.[6] applied single event kinetics for the hydrocracking of C_8-C_{12} paraffins on Pt/USY zeolites. Recently, Park et al.[15] applied the single event kinetics for modeling the methanol to olefin process over HZSM-5 catalyst.

CHAPTER II

CHEMISTRY AND MECHANISM OF HYDROCRACKING REACTIONS

2.1 Chemistry of the Hydrocracking Reactions

The hydrocracking of oil fractions is carried out on bifunctional catalysts consisting of a metal and an acid function. The metal function serves for the hydrogenation/dehydrogenation and the acid function is responsible for the isomerization and cracking reactions. For second stage hydrocracking, Pt-loaded zeolites are found to be the best catalyst and are predominantly used nowadays. Zeolites are alumino-silicates in which aluminum and silicon atoms are tetrahedrally coordinated to four oxygen atoms. Each of the oxygen atoms bridges between two silicon atoms. The geometrical arrangement of the silicon atoms relative to each other forms a secondary structure superposed on the primary tetrahedron structure. Because the silicon atoms are interlinked by bridging oxygen atoms, rings of alternating silicon and oxygen atoms are formed. Zeolites can be considered to be structured assemblies of such rings. Because of the large variation in ring sizes and possible ways of connecting them, numerous structures can be formed (so far 133 structures have been reported). The arrangement of the rings may give rise to pores and cages as can be seen in Figure 2.1, showing the frameworks of two zeolites.[16]

Zeolites have a very high resistance for deactivation by feed impurities and their structure with molecular size pores and voids make them good catalyst providing higher selectivities for the desired products. The shape selectivity of zeolites also suppresses the deactivation of catalyst from the polymerization of alkenes because the transition states of polymerization reactions are too bulky to fit the pores of the zeolites. Addition of Pt also helps in hydrogenating the coke precursors to increase the catalyst life.[16]

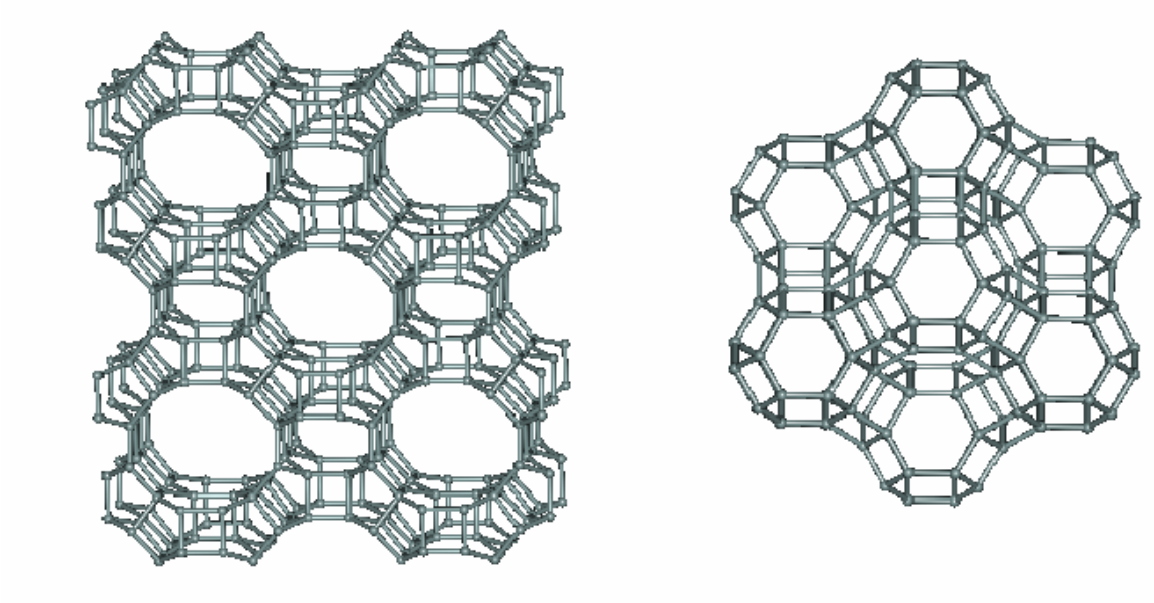

(a) **(b)**

Figure 2.1 Zeolite structures for (a) Mordenite (b) Faujasite

The reactions in hydrocracking take place through the carbenium ion chemistry along with the chemistry of hydrogenation and dehydrogenation. The reaction process is schematically represented in Figure-2.2[17] and the various types of reactions for paraffinic feeds are summarized in Figure-2.3.[5] The feed molecules in the liquid phase are first physically adsorbed in the zeolite cages.[18] The adsorbed paraffin molecules are dehydrogenated at the metal sites of the catalyst to produce olefin intermediates. The olefins are rapidly protonated on the Bronsted acid sites yielding the alkyl carbenium ions. These carbenium ions are isomerized by hydride shift, methyl shift and protonated cyclo propane (PCP) steps. The isomerized carbenium ions having a higher degree of branching after PCP steps are cracked at the carbon-carbon bond in the β-position with respect to the carbon atom bearing the positive charge.

The products of β-scission are a smaller carbenium ion and an olefin. The carbenium ion can further crack, or deprotonate at the acid sites to produce an olefin molecule. Similarly, the olefin molecule can protonate to yield another carbenium ion, or alternatively can hydrogenate at the metal site of the catalyst to produce paraffins. The probability of either undergoing protonation or hydrogenation depends on the relative strength of the acid/metal functions of the catalyst. Figure 2.4 depicts the sequence of various physical and chemical phenomena taking place in hydrocracking of paraffinic feeds.

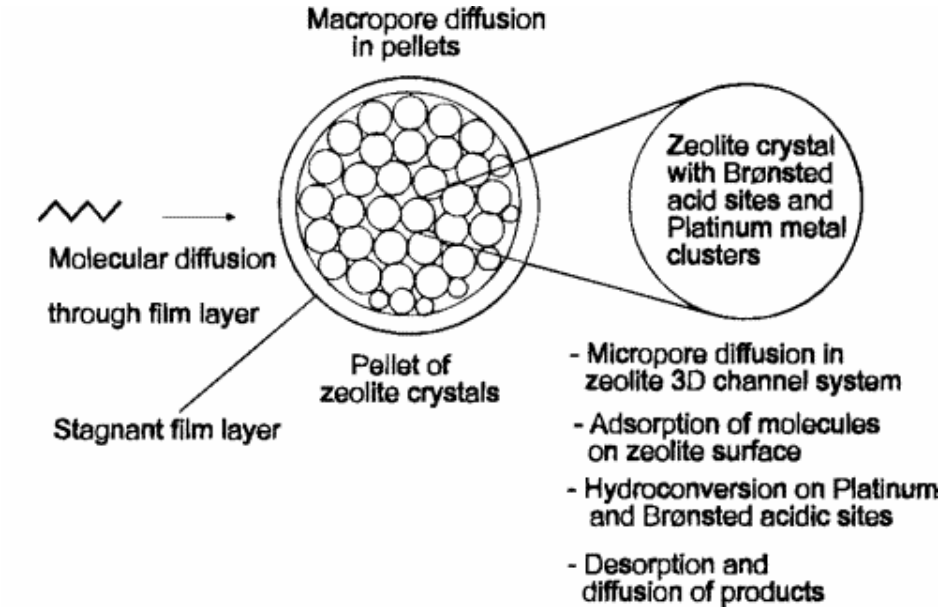

Figure 2.2 Schematic representation of the reaction scheme of hydrocarbon molecule at the catalyst surface[17]

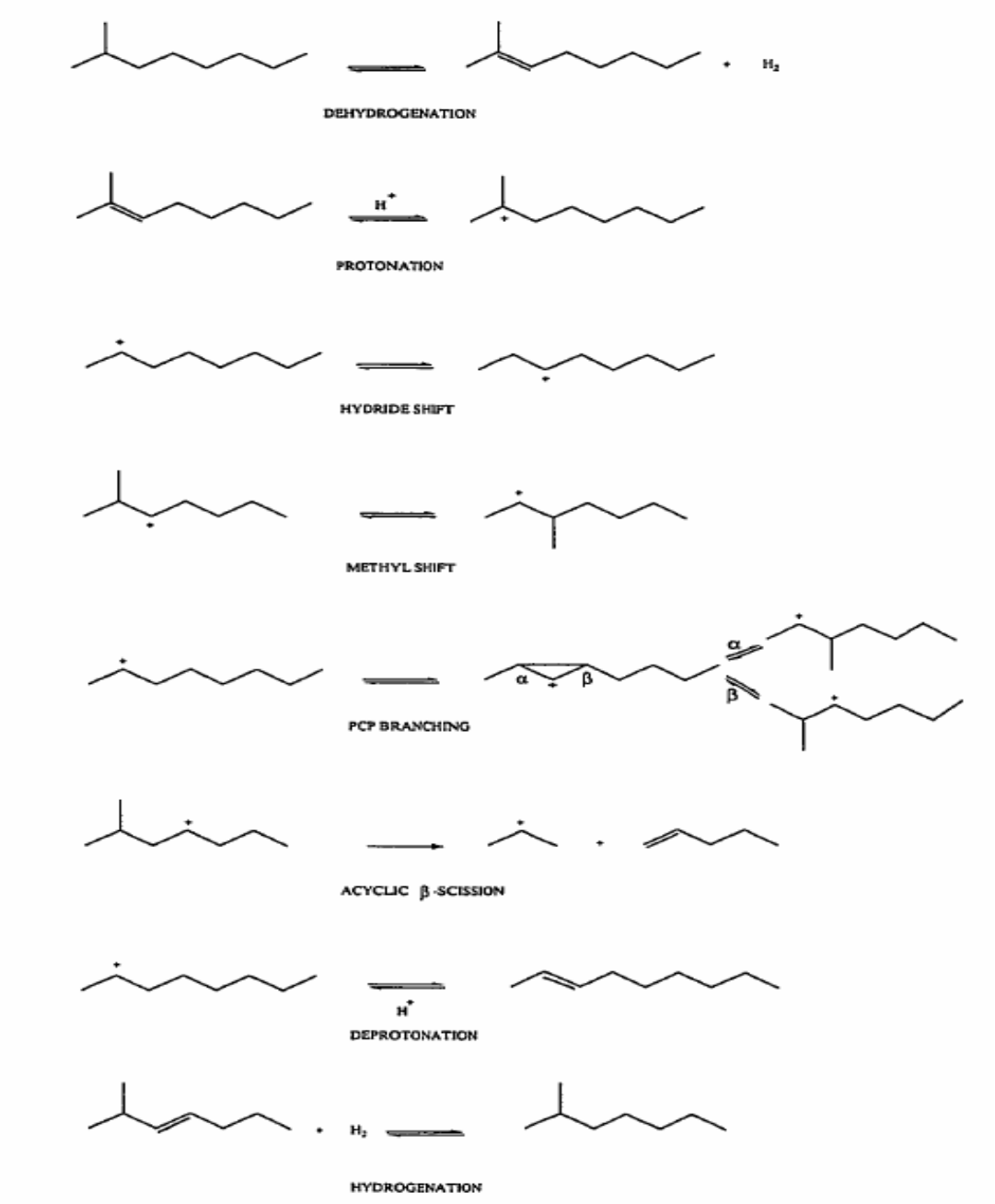

Figure 2.3 List of elementary steps for the hydrocracking of paraffins[10]

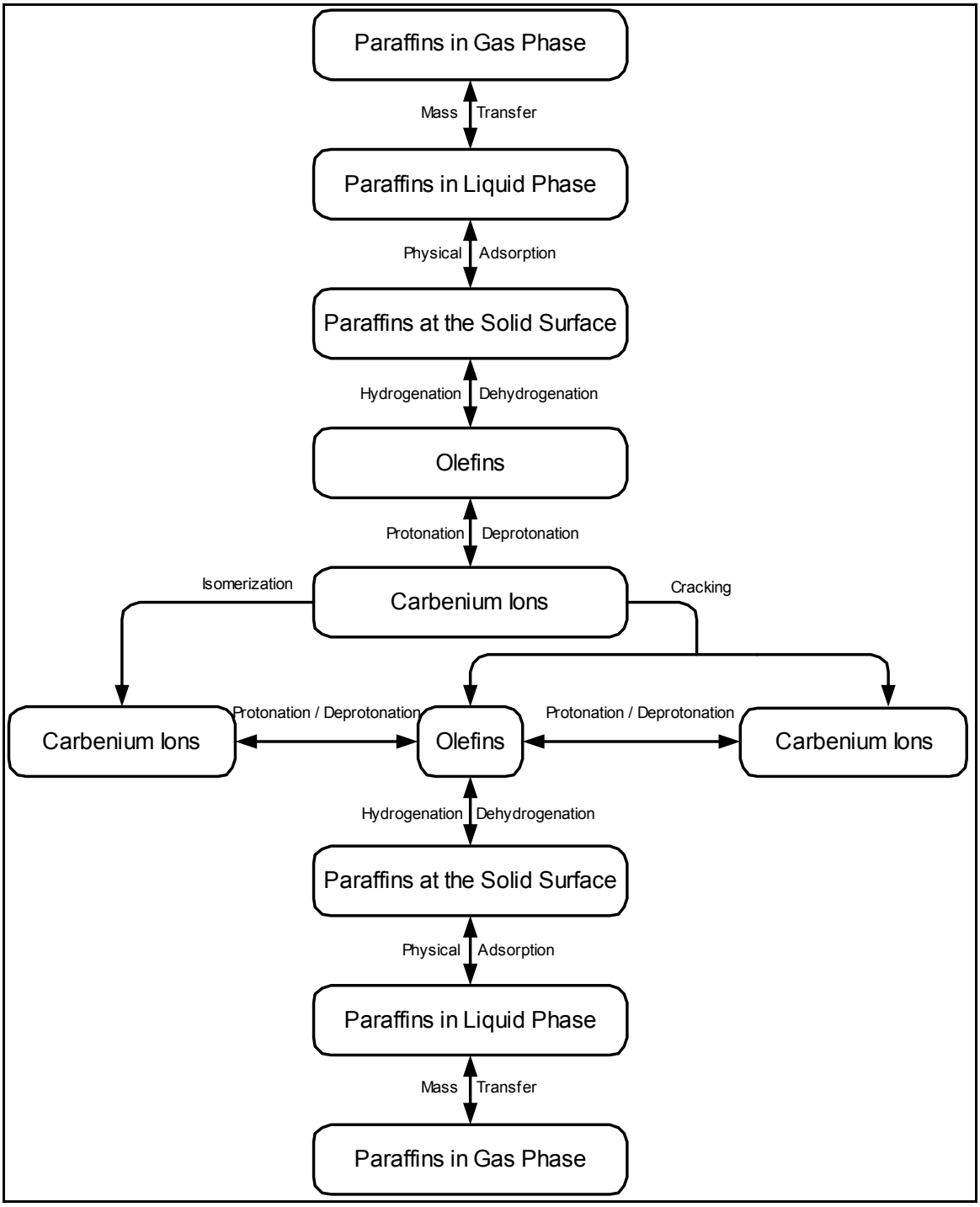

Figure 2.4 Schematic representation of various physical and chemical phenomena taking place in hydrocracking of paraffins

2.2 Mechanism of Acid Catalyzed Steps

2.2.1 Isomerization Steps

Isomerization reactions are usually classified into two groups, namely isomerization reactions in which the degree of branching remains unchanged (alkyl shift and hydride shift) and isomerization reactions in which the degree of branching changes through a protonated cyclo propane intermediate. Nowadays it is generally accepted that alkyl shift and hydride shift isomerization also proceeds through cyclization of the carbenium ion into a protonated cyclopropane (PCP), followed by opening of the cyclopropane ring:[19]

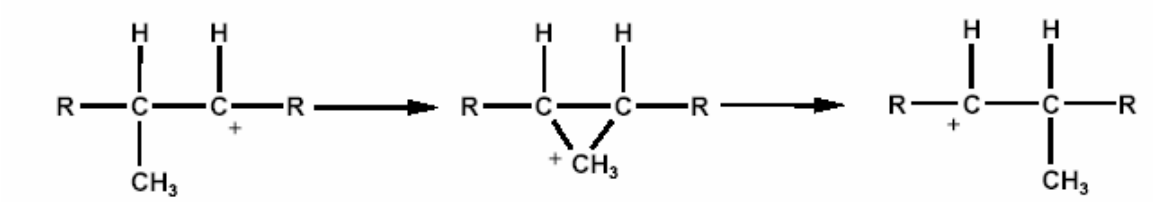

Figure 2.5 Mechanism of methyl shift steps

However, the difference in case of PCP steps with change in degree of branching is that the opening of the cyclopropane ring is preceded by a corner-to-corner proton jump,[19] which itself proceeds via an edge-protonated cyclopropane intermediate or transition state.[20]

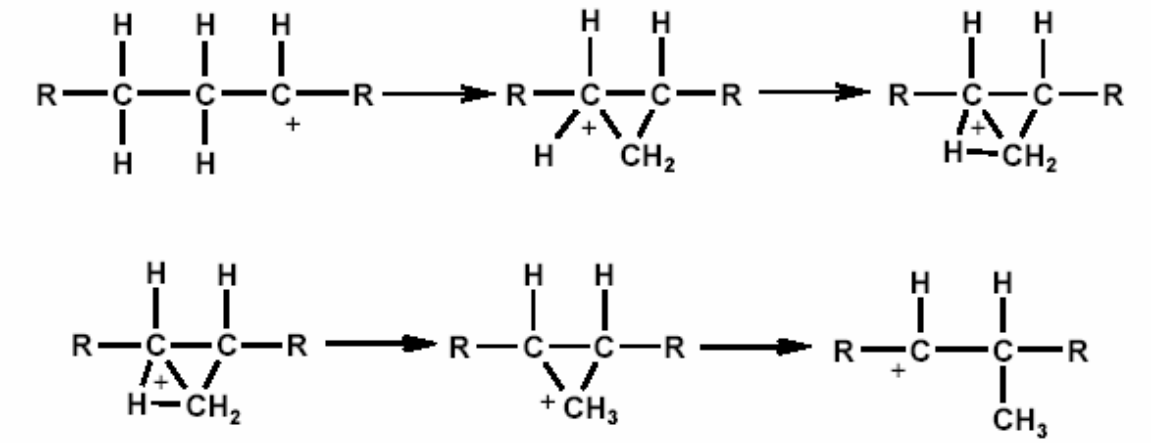

Figure 2.6 Mechanism of PCP steps

Because the activation energy of the proton jump is considerable in these steps, they are slower as compared to the isomerization steps without change in the degree of branching.[19]

There is no reason to exclude protonated cycloalkanes with rings containing more than three carbon atoms as possible intermediates in skeletal isomerization. Indeed, studies of the distribution of products resulting from the isomerization of a series of *n*-alkanes have provided evidence for the existence of protonated cyclobutanes, cyclopentanes etc.[21,22] However, the contribution of protonated cycloalkanes to the formation of branched isomers rapidly decreases with increasing ring size.[22]

2.2.2 Cracking Steps

Cracking of carbenium ions proceeds via so-called β-scission, which involves the transfer of the two electrons of the C-C bond in the β position of the charged carbon atom toward the C-C bond in the α position. As a result the fragment containing the α C-C bond is an alkene, while the other fragment is a carbenium ion because the carbon atom originally in the γ position loses an electron. Depending on the skeletal configuration of the starting carbenium ion, five types of β-scission steps can be distinguished as shown in Figure 2.7.

The rate of β-scission steps decreases in the following order:

$$Cr(t;t) >> Cr(s;t), Cr(t;s) > Cr(s;s) >> Cr(s;p)$$

This order can be explained by considering the stabilities of the carbenium ions that are involved in respective steps. The order of stabilities of the carbenium ions is as follows:

Tertiary > Secondary > Primary >Methyl

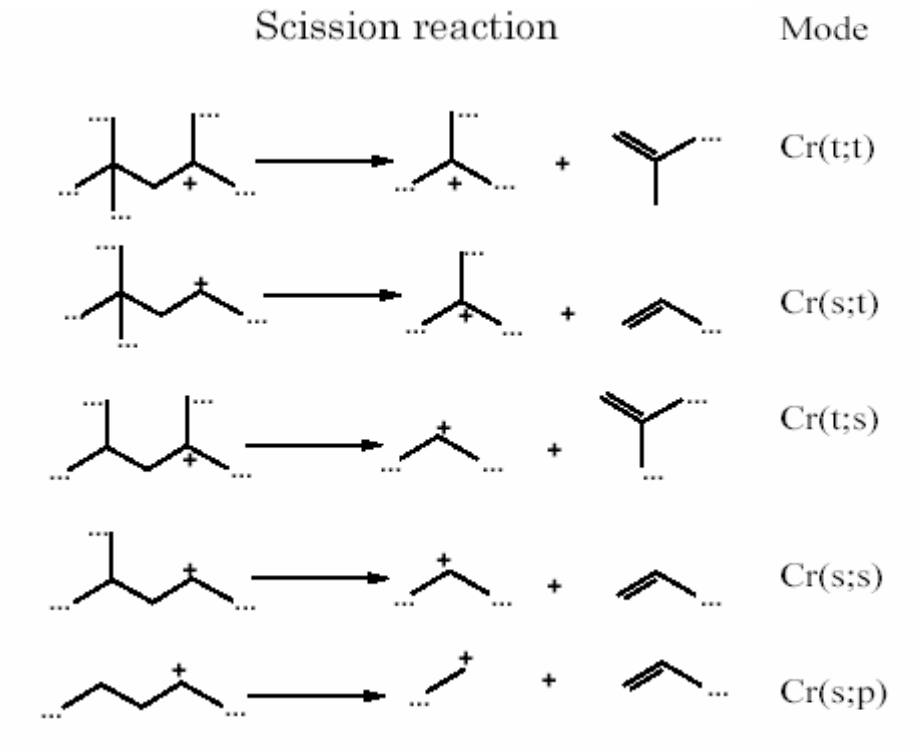

Figure 2.7 Type of β-scission steps. The dots represent the alkyl groups[16]

Alkyl groups presumably stabilize the positive charge because overlap of the vacant *p* orbitals of the positively charged carbon atom and a neighboring C-H σ-bond leads to charge delocalization (hyperconjugation), and the higher polarizability of an alkyl group compared to that of a hydrogen atom allows more electron density to shift towards the charge. As a result, tertiary carbenium ions are the most stable followed by secondary, primary and methyl carbenium ions, in the decreasing order of stability.

Cr(s;p) β-scission is therefore the slowest mode since it yields a primary carbenium ion. Cr(t;t) β-scission is much faster than Cr(t;s) and Cr(s;s) β-scission because it produces a tertiary carbenium ion, whereas the other modes produce only secondary carbenium ions. At first sight it seems surprising that Cr(s;t) cleavage is not the fastest mode of β-scission because in this step a secondary carbenium ion is converted into a more stable

tertiary ion. However, since the reacting alkane rapidly isomerizes to a more stable tertiary carbenium ion, its equilibrium concentration is very low.[16]

CHAPTER III

SINGLE EVENT KINETICS AND REACTION NETWORK GENERATION

3.1 Theory of Single-Event Kinetics

In single event kinetics, the effect of molecular structure on the rate coefficient of an elementary step is described with the help of transition state theory and statistical thermodynamics.[10] The rate coefficient of an elementary step is given by transition state theory as,

$$k = \left(\frac{k_B T}{h}\right)\exp\left(\frac{\Delta S^{o\ddagger}}{\mathrm{R}}\right)\exp\left(\frac{-\Delta H^{o\ddagger}}{\mathrm{RT}}\right) \tag{3.1}$$

According to statistical thermodynamics, the entropy of a species can be determined by adding the contribution from different types of motion viz. transnational, rotational, vibrational and electronic, i.e.,

$$S^o = S^o_{Trans} + S^o_{Vib} + S^o_{Rot} + S^o_{Elec} \tag{3.2}$$

where $$S^o_{Rot} = S^o_{ExtRot} + S^o_{IntRot} \tag{3.3}$$

The rotational part of the entropy is composed of an intrinsic term, $\hat{S}^o$ and a contribution from the symmetry of the molecule, $R\ln\sigma$, i.e.,

$$S^o_{ExtRot} = \hat{S}^o_{ExtRot} - R\ln(\sigma_{Ext}) \tag{3.4}$$

and $$S^o_{IntRot} = \hat{S}^o_{IntRot} - R\ln(\sigma_{Int}) \tag{3.5}$$

For racemic mixtures of optically active species, an additional entropy contribution of $R\ln(2^n)$ due to the mixing of different enantiomers has to be considered, where *n* is the number of chiral centers in the molecule.

$$S^o_{Rot} = \hat{S}^o_{Rot} - R\ln\left(\frac{\sigma_{Ext}\sigma_{Int}}{2^n}\right) \tag{3.6}$$

$$\text{where} \quad \hat{S}^o_{Rot} = \hat{S}^o_{ExtRot} + \hat{S}^o_{IntRot} \tag{3.7}$$

$$\text{and} \quad \left(\frac{\sigma_{Ext}\sigma_{Int}}{2^n}\right) = \text{Global Symmetry Number, } \sigma_{gl} \tag{3.8}$$

The global symmetry number σ_{gl} quantifies all the symmetry contributions of a species. Using the above equations, the standard entropy of activation for an elementary step can be written as:

$$\Delta S^{o\ddagger} = \Delta S^{o\ddagger}_{Trans} + \Delta S^{o\ddagger}_{Vib} + \Delta S^{o\ddagger}_{Elec} + \Delta \hat{S}^{o\ddagger}_{Rot} + R\ln\left(\frac{\sigma^R_{gl}}{\sigma^{\ddagger}_{gl}}\right) \tag{3.9}$$

The last term of equation (3.9) gives the difference in standard entropy between reactant and activated complex due to the symmetry changes. Equation (3.9) can also be written as,

$$\Delta S^{o\ddagger} = \Delta \hat{S}^{o\ddagger} + R\ln\left(\frac{\sigma^R_{gl}}{\sigma^{\ddagger}_{gl}}\right) \tag{3.10}$$

$$\text{where} \quad \Delta \hat{S}^{o\ddagger} = \Delta S^{o\ddagger}_{Trans} + \Delta S^{o\ddagger}_{Vib} + \Delta S^{o\ddagger}_{Elec} + \Delta \hat{S}^{o\ddagger}_{Rot} \tag{3.11}$$

Using equation (3.1) and (3.10), the effect of changes in symmetry in going from reactant to activated complex on the rate coefficient of an elementary step can be factored out. i.e.,

$$k = \left(\frac{\sigma_{gl}^{R}}{\sigma_{gl}^{\ddagger}}\right)\left(\frac{k_B T}{h}\right)\exp\left(\frac{\Delta\hat{S}^{o\ddagger}}{\mathrm{R}}\right)\exp\left(\frac{-\Delta H^{o\ddagger}}{\mathrm{RT}}\right) \tag{3.12}$$

The rate coefficient of an elementary step k, can now be written as a multiple of the single-event rate coefficient $\tilde{k}$ [11] as

$$k = n_e \tilde{k} \tag{3.13}$$

where the number of single events n_e and single event rate coefficient $\tilde{k}$ can be defined as

$$n_e = \left(\frac{\sigma_{gl}^{R}}{\sigma_{gl}^{\ddagger}}\right) \tag{3.14}$$

$$\tilde{k} = \left(\frac{k_B T}{h}\right)\exp\left(\frac{\Delta\hat{S}^{o\ddagger}}{\mathrm{R}}\right)\exp\left(\frac{-\Delta H^{o\ddagger}}{\mathrm{RT}}\right) \tag{3.15}$$

Since the difference in symmetry, i.e. the difference in structure between the reactant and the activated complex has been factored out by introducing the number of single-events n_e, the single-event rate coefficient $\tilde{k}$ is independent of the structure of the reactant.

3.2 Generation of the Reaction Network

Considering the large number of reaction pathways in the hydrocracking of hydrocarbons, the complete reaction network has been generated using a computer program. The development of the reaction network has been done by using the Boolean

relation matrices and characterization vectors.[12] The methodology and procedure for generating the reaction network is given in the following sections.

3.2.1 Representation of Chemical Species

To generate the reaction network by computer, it is required to represent the chemical species in a mathematical way. For this purpose, a hydrocarbon is represented by a binary relation matrix M and a characterization vector N. The first step in representing a molecule in this way is numbering all the carbon atoms in an arbitrary, but standardized manner. A carbon-carbon bond between atoms *i* and *j* is represented by a 1 on the *(i, j)* entry of the matrix M. All other elements of matrix M are set to zero. This produces a *(n* x *n)* symmetric matrix showing the bonding in the molecule having *n* carbon atoms.

The characterization vector N has *(2n+1)* elements. The first *n* elements are the sum of entries of respective columns of the matrix M and thus show the type i.e. primary, secondary, tertiary etc of the respective carbon atoms. The values of the next *n* elements are used to characterize the nature of each carbon atom. These values are assigned arbitrarily based on certain predefined rules. For example, in the reaction network of hydrocracking of paraffins, a carbon atom can be either saturated or olefinic. An index of 8 is assigned for saturated carbon atoms and 7 for double bonded carbon atoms. The last i.e., $(2n+1)^{th}$ element shows the number of the carbon atom carrying the positive charge to represent the carbenium ion species. A value of zero is assigned to this element in case of the molecular species.

As an example, 2-methyl-5-hexyl is a secondary carbenium ion having 7 carbon atoms. The Boolean relation matrix and characterization vector of this carbenium ion are given in Figure-3.1.

It can be seen that carbon atom 2 is connected to carbon atoms 1, 3 & 7, and therefore (2, 1), (2, 3) and (2, 7) entries of the Boolean matrix in Figure-3.1 are assigned a value 1. All other elements of second row are set to zero. Similarly, based on the bonding between the carbon atoms the entire Boolean matrix is constructed.

Since there are 7 carbon atoms in this carbenium ion, the first 7 entries of the characterization vector are assigned based on the type of each carbon atom. For example 2 is a tertiary carbon atom and therefore, second element of the characterization vector is assigned a value of 3. Since all the carbon atoms in the above carbenium ion are saturated in nature, the next 7 entries (i.e., from 8 to 14) of the characterization vector are assigned a value of 8, the index representing the saturated carbon atoms. The last element is assigned a value of 5, showing the location of the positive charge in the carbenium ion.

	1	2	3	4	5	6	7
1	0	1	0	0	0	0	0
2	1	0	1	0	0	0	1
3	0	1	0	1	0	0	0
4	0	0	1	0	1	0	0
	0	0	0	1	0	1	0
	0	0	0	0	1	0	0
	0	1	0	0	0	0	0

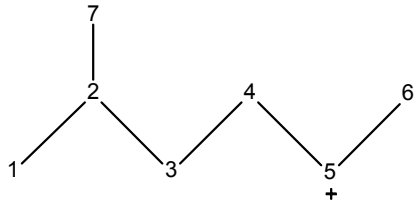

Location of the positive charge

1	3	2	2	2	1	1	8	8	8	8	8	8	8	5

Type of carbon atom

Nature of carbon atom

Figure 3.1 Boolean relation representation of 2-methyl-5-hexyl and characterization vector

3.2.2 Standardization of Labeling

As discussed in the previous section, the Boolean relation matrices and the characterization vectors are constructed based on the numbering of the carbon atoms in a molecule. Therefore depending on the numbering, a single species can be represented by several different Boolean relation matrices and their corresponding characterization vectors. To avoid the non-uniqueness of Boolean relation matrices, the numbering of the molecule has to be done in a standardized fashion. Arbitrary rules for labeling the species in a standard way are established to make sure that there is only one way to label any species involved in the reaction network.[12]

3.2.3 Generation of Elementary Steps

All different types of elementary steps encountered in hydrocracking i.e., hydride shift, methyl shift, PCP isomerization, β-scission etc. can be generated mathematically by simple matrix operations on the Boolean relation matrices and characterization vectors. As an example, generation of the hydride shift elementary steps of any carbenium ion starts from identifying the location of the positive charge from the characterization vector, which is 5 for the above considered carbenium ion. Since the positive charge shifts to the nearest carbon atom in a hydride shift step, the atoms connected to carbon atom 5 are then determined from the Boolean relation matrix. In this case, the latter is connected to carbon atoms 4 and 6 leaving out maximum two possible hydride shift steps. The next step is to determine the type of the prospective carbon atoms (whether they are primary, secondary or tertiary) where the positive charge will migrate if a particular hydride shift elementary step takes place. In this case, carbon atom 6 is primary and therefore the resulting carbenium ion will also be primary, which is highly unstable. Because of their unstable nature, the generation of the primary carbenium ions is not considered in the network generation program (rule-1). The details of the rules considered for the network generation program are described in the following section. Therefore the only possible hydride shift for 2-methyl-5-hexyl is the generation of 2-methyl-4-hexyl which will be a secondary carbenium ion. As the skeleton of the

molecule does not undergo any change during hydride shift, the Boolean relation matrix for the product carbenium ion will be same as for the reactant. The only change will come in the last entry of the characterization vector, in which the location of the positive charge will be changed from 5 to 4. The resulting carbenium ion and its characterization vector are shown in Figure 3.2.

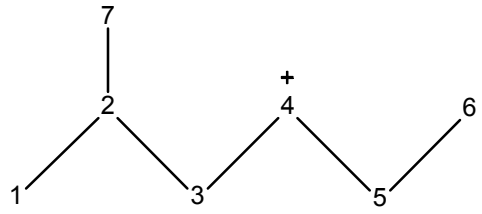

1	3	2	2	2	1	1	8	8	8	8	8	8	8	4

Figure 3.2 2-methyl-4-hexyl and its characterization vector

The possibilities for the β-scission in a carbenium ion can be determined from the matrix obtained by squaring of the Boolean relation matrix of the reactant carbenium ion and replacing its diagonal entries from 1 to 0 i.e., from the matrix $M \otimes M - I$. This matrix gives all the (1, 3) locations of the carbon atoms. As an illustration, the Boolean relation matrix shown in Figure 3.3 contains the information about the β carbons for 2-methyl-5-hexyl. The entries in the third row of this matrix show that carbon atoms 1, 5 & 7 are the β carbons for the carbon atom 3, as can be seen from the structure of the molecule also.

	1	2	3	4	5	6	7
1	0	0	1	0	0	0	1
2	0	0	0	1	0	0	0
3	1	0	0	0	1	0	1
4	0	1	0	0	0	1	0
5	0	0	1	0	0	0	0
6	0	0	0	1	0	0	0
7	1	0	1	0	0	0	0

Figure 3.3 β positions of 2-methyl-5-hexyl carbenium ion

Since the positive charge in 2-methyl-5-hexyl is located on carbon atom 5, the only possibility of β scission for this carbenium ion is for the bond between carbon atoms 3 and 4. However, if this bond breaks, the resulting carbenium ion will be primary, and therefore this β scission step will not be considered in the network generation program.

A simplified algorithm for the generation of reaction network for paraffins is given in Figure 3.4.

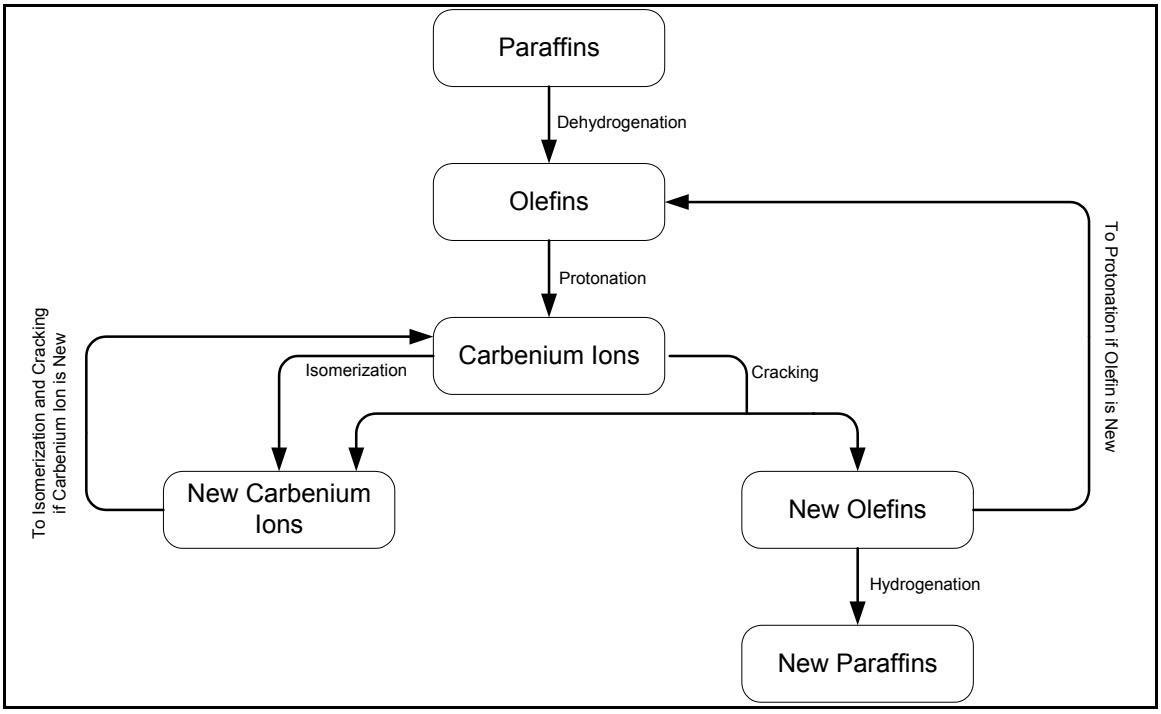

Figure 3.4 Algorithm for the network generation for paraffins

3.3 Rules for Generating the Reaction Network

The generation of the reaction network for paraffins is based on certain predefined rules. These rules are derived from the carbenium ion chemistry and from the experimental evidences obtained from the hydrocracking of paraffinic species. The summary of these rules and their explanation is given as follows:

1) Generation of primary and methyl carbenium ions is not considered. This rule came from the stability study of the carbenium ions. Considering the high energy required to form the primary and methyl carbenium ions and their highly unstable nature as compared to secondary and tertiary carbenium ions, no elementary step generating primary and methyl carbenium ions has been considered in the reaction network.[10]

2) It has been found from analysis of oil fractions that the species with more than three side chains are present in very low concentrations. Therefore, species having more than three side chains are not considered in the network generation.[11]

3) Species with only methyl side chains are considered. Therefore, no species with ethyl or longer side chains are generated in the reaction network. This rule is also based on the experimental studies of hydrocracking.[5]

4) The contribution of protonated cycloalkanes to the formation of branched isomers rapidly decreases as the ring size increases above three carbon atoms[16] and therefore, only protonated cyclo propane (PCP) elementary steps are considered for the isomerization steps introducing the degree of branching. This rule makes sure that no species having ethyl or bigger side chains are generated.

5) Bimolecular hydrogen transfer steps are not considered.[5]

3.4 Reaction Network for n-Hexadecane

The reaction network has been generated for the hydrocracking of n-hexadecane and for a heavy paraffinic feed up to C_{33}. The number of different type of elementary steps, and the number of olefin species and carbenium ions involved for these two feedstocks are summarized in Table-3.1.

TABLE 3.1: Results of Network Generation for C_{16} and C_{33} Feedstocks

Type of Elementary Steps	Number of Elementary Steps	
	C_{16} Feed	C_{33} Feed
Protonation	12831	836,693
Deprotonation	12,845	837,015
Hydride shift	10,470	761,712
Methyl shift	2,670	89,960
Protonated cyclo propane	8,485	275,176
β- scission	2,335	85,602
Total Elementary Steps	49,636	2,886,158 (~3 Million)
Carbenium Ions Involved	6,167	396,354
Olefins Involved	7,601	448,395

CHAPTER IV

MODEL PARAMETERS AND DEVELOPMENT OF RATE EXPRESSIONS

4.1 Kinetic Parameters in the Model

In a complex process like hydrocracking of heavy paraffins where several thousands elementary steps are taking place simultaneously, involving thousands of products and intermediate species, identification of the independent rate parameters is of utmost importance. Since the reactions take place at the surface of the solid catalyst, the physical adsorption of the reacting species and intermediates on the catalyst surface also needs to be modeled in addition to the rate parameters.[23]

The present chapter provides the detailed procedure and methodology to build up the kinetic model with appropriate simplifying assumptions in such a way that the model contains a tractable number of independent parameters.

As discussed in Chapter III, with the application of single event concept, the rate coefficient of an elementary step can be written as the number of single events for that particular step multiplied by the single event rate coefficient, i.e.,

$$k = n_e \tilde{k} \tag{4.1}$$

The number of single events factors out the effect of the structure of the reactant and transition state from the rate coefficient of an elementary step. Consequently, the single event rate coefficient is only a function of the difference in intrinsic entropy and energy levels between the reactant and the transition state. The same conclusion can also be drawn with the help of the Benson's group theory provided that the heat of formation and the intrinsic entropy of transition states can be calculated using group contribution

theory.[5] Therefore, the above equation means that all the elementary steps of a certain type in which the intrinsic entropy and energy changes from reactants to the transition states can be justified to be same will have only one single event rate coefficient. The rate coefficients of different elementary steps of that type can then be obtained by multiplying the single event rate coefficient with the number of single events of the respective elementary steps.

As discussed in Chapter II, the hydrocracking of paraffins takes place through the carbenium ion intermediates and their stability/reactivity depends on the type of the carbon atom having the positive charge, whether it is secondary or tertiary. Therefore, the different type of isomerization and cracking elementary steps occurring in hydrocracking are categorized primarily based on the type of the reactant and product carbenium ions. The details of different type of elementary steps and the number of single event rate coefficient required for their modeling are discussed below:

4.1.1 Isomerization Steps

Based on the energy levels of the reactant and the product carbenium ions, only four single event rate coefficient $\tilde{k}_{isom}(s;s)$, $\tilde{k}_{isom}(s;t)$, $\tilde{k}_{isom}(t;s)$ and, $\tilde{k}_{isom}(t;t)$ are required for isomerization. The subscripts *isom* can be hydride shift (HS), methyl shift (MS) or protonated cyclo propane (PCP). It has been argued that these rate coefficients can be used irrespective of the carbon number of the feed. It should be noted that the degree of branching of a carbenium ion in hydride shift and methyl shift isomerization remains the same in contrast to PCP isomerization in which the degree of branching changes. Because of lesser changes in the molecular structure in HS and MS isomerization as compared to PCP, the former isomerization steps are much faster than the latter,[16] and thus for any particular carbon number, all the isomers with same degree of branching rapidly reach reaction equilibrium. Because of this equilibrium between the isomers of same degree of branching, a partial lumping is introduced in this kinetic model based on the degree of branching per carbon number (discussed in Chapter V in detail). This

eliminates the need to estimate the rate parameters for HS and MS leaving out only four rate parameters for PCP isomerization, namely $\tilde{k}_{PCP}(s;s)$, $\tilde{k}_{PCP}(s;t)$, $\tilde{k}_{PCP}(t;s)$ and, $\tilde{k}_{PCP}(t;t)$. The further reduction in the number of isomerization parameters has been discussed later using the thermodynamic relationships.

4.1.2 Cracking Steps

Until recently, the elementary steps for cracking were modeled similar to that for isomerization steps, i.e., four single event rate coefficients $\tilde{k}_{Cr}(s;s)$, $\tilde{k}_{Cr}(s;t)$, $\tilde{k}_{Cr}(t;s)$ and, $\tilde{k}_{Cr}(t;t)$ were used irrespective of the type of the olefin produced for any carbon number of the reactant carbenium ion. Govindhakannan J.[24] on the other hand introduced the dependency of the produced olefin on the single event rate coefficient of cracking. The basis of introducing this dependency, however, is thus far empirical in nature. He suggested that for a particular type of reactant and product carbenium ion, two different single event cracking rate coefficients should be used depending upon whether a normal or an iso-olefin is produced as the second product of cracking. This modification leads to a total of eight single event rate coefficients listed below:

$$\tilde{k}_{Cr}(s;s,no),\tilde{k}_{Cr}(s;s,io)$$

$$\tilde{k}_{Cr}(s;t,no),\tilde{k}_{Cr}(s;t,io)$$

$$\tilde{k}_{Cr}(t;s,no),\tilde{k}_{Cr}(t;s,io)$$

$$\tilde{k}_{Cr}(t;t,no),\tilde{k}_{Cr}(t;t,io)$$

'no' and *'io'* in the above rate coefficient signify whether the produced olefin is normal or iso. Later it was found that there is no possible elementary steps in which a tertiary carbenium ion can produce a normal olefin on cracking. This reduced the number of rate coefficient for cracking from 8 to 6 eliminating $\tilde{k}_{Cr}(t;s,no)$ and $\tilde{k}_{Cr}(t;t,no)$. The remaining 6 single event rate coefficients are estimated from the experimental data.

4.1.3 Protonation / Deprotonation Steps

Protonation/deprotonation steps are very fast as compared to PCP and cracking steps, and therefore, it is assumed that protonation/deprotonation steps are always at reaction equilibrium.[10] For any arbitrary pair of olefin isomers, a reversible reaction pathway can be found which connects both olefins via a series of carbenium ions. As an example, the following two olefins O_1 and O_2 are connected through the carbenium ion R_1^+ as follows:

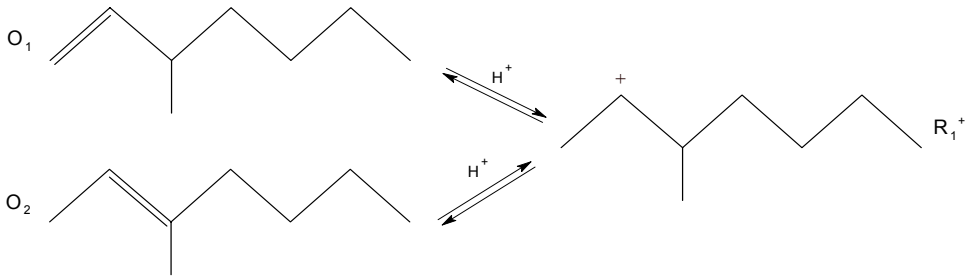

Figure 4.1 Reaction pathway between two olefins through a carbenium ion

The equilibrium constant for the isomerization between these two olefins can be expressed as the product of the protonation/deprotonation equilibrium constants for the pathways connecting the olefins through the common carbenium ion. i.e.,

$$K_{isom}^{(O_1 \rightleftarrows O_2)} = K_{pr/de}^{(O_1 \rightleftarrows R_1^+)} K_{de/pr}^{(R_1^+ \rightleftarrows O_2)} \tag{4.2}$$

Expressing the equilibrium constant by the ratio of the forward to the backward rate coefficient and identifying that R_1^+ is a secondary carbenium ion, the above equation becomes,

$$K_{isom}^{(O_1 \rightleftarrows O_2)} = \frac{k_{pr}(O_1;s)}{k_{de}(s;O_1)} \frac{k_{de}(s;O_2)}{k_{pr}(O_2;s)} \tag{4.3}$$

To simplify this equation, it is assumed that the activated complex in a protonation/deprotonation step has a structure resembling the olefin structure but with the double bond not yet broken/formed completely. This line of thought makes it possible to consider that the differences in the stability between the olefin isomers are maintained in the corresponding activated complexes. It is equivalent to saying that the activation enthalpy and entropy of the protonation of an olefin are independent of the nature of the reacting olefin. This means that the rate coefficient for protonation of olefins depends only on the type of the carbenium ion produced, not on the reactant olefin. Therefore, $k_{pr}(O_j;m)$ in the above equation reduces to $k_{pr}(m)$, where *m* can be either *s* or *t*. In this way there are only two protonation rate coefficients namely, $k_{pr}(s)$ and $k_{pr}(t)$. Moreover, since the structure of the transition state has been assumed similar to the structure of the olefin, both of them will have same symmetry number and thus the number of single event for any protonation step becomes one. Therefore, the single event rate coefficient for protonation $\tilde{k}_{pr}(m)$ becomes equal to rate coefficient for the protonation elementary step $k_{pr}(m)$. As previously assumed in the case of isomerization and cracking, the single event rate coefficients for protonation are also independent of the number of carbon atoms in the feed leaving only two rate coefficients for all the protonation steps. Incorporating the above changes in protonation rate coefficients and expressing the isomerization equilibrium constant and deprotonation rate coefficients in terms of single event isomerization equilibrium constant and single event deprotonation coefficient, respectively, results in the following equation,

$$(\sigma_{O_1}/\sigma_{O_2})\,\tilde{K}_{isom}^{(O_1 \rightleftarrows O_2)} = \frac{\tilde{k}_{pr}(s)}{(\sigma_{R_1^+}/\sigma_{O_1})\,\tilde{k}_{de}(s;O_1)} \frac{(\sigma_{R_1^+}/\sigma_{O_2})\,\tilde{k}_{de}(s;O_2)}{\tilde{k}_{pr}(s)} \tag{4.4}$$

The above equation can be simplified as

$$\tilde{K}_{isom}^{(O_1 \rightleftarrows O_2)} = \frac{\tilde{k}_{de}(s;O_2)}{\tilde{k}_{de}(s;O_1)} \tag{4.5}$$

This expression can be generalized for any pair of olefins for which an isomerization pathway via one and the same carbenium ion of type *m* exists. In other words, for each of two olefins with a common skeleton structure and adjacent double bonds, one can write,

$$\tilde{K}_{isom}^{(O_i \rightleftarrows O_j)} = \frac{\tilde{k}_{de}(m;O_j)}{\tilde{k}_{de}(m;O_i)}$$

The same expression can also be derived for the more general case of two olefins with a different skeleton structure. The detailed derivation can be found in reference [10]. Above equation can be rewritten as follows:

$$\tilde{k}_{de}(m;O_j) = \tilde{K}_{isom}^{(O_r \rightleftarrows O_j)} \tilde{k}_{de}(m;O_r) \tag{4.6}$$

where O_r represents the reference olefin isomer with the double bond preferably in such a position that both a secondary as well as a tertiary carbenium ion can be formed by protonation. The reference olefins for each carbon number are judiciously selected from a homologous series[14] and the rates of deprotonation of the carbenium ions are assumed to be equal in the homologous series. The single event isomerization equilibrium constants $\tilde{K}_{isom}^{(O_r \rightleftarrows O_j)}$ for every olefin species involved in the reaction network with the reference olefin for each carbon number are calculated using Benson's group contribution method.[5] This technique enables the calculation of all the single event deprotonation coefficients using only two independent single event deprotonation rate coefficients namely, $\tilde{k}_{de}(s;O_r)$ and $\tilde{k}_{de}(t;O_r)$ for any carbon number.

4.1.4 Thermodynamic Constraints

If the double bond in an olefin is not in the terminal position, the olefin protonation will always give two carbenium ions. If the double bond in the olefin is located between a secondary and tertiary carbon atom, the product carbenium ions will be of different type, i.e., secondary and tertiary. These two carbenium ions can be interconverted through a single 1-2 hydride shift elementary step as illustrated in the following example,

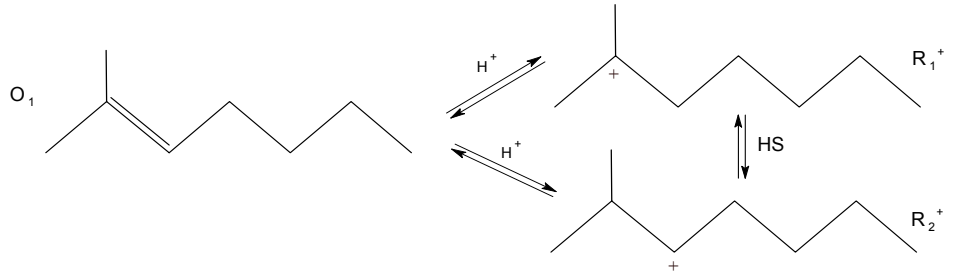

Figure 4.2 Reaction pathway between two carbenium ions through an olefin

Parallel to equation (4.2), the following equation can be written for the above reactions:

$$K_{HS}^{(R_1^+ \rightleftarrows R_2^+)} = K_{de/pr}^{(R_1^+ \rightleftarrows O_1)} K_{pr/de}^{(O_1 \rightleftarrows R_2^+)} \tag{4.7}$$

Similar to the procedure given in section 4.1.3, this equation can be written in terms of the single event rate coefficients as

$$\frac{\tilde{k}_{HS}(t;s)}{\tilde{k}_{HS}(s;t)} = \frac{\tilde{k}_{pr}(s)}{\tilde{k}_{pr}(t)} \frac{\tilde{k}_{de}(t;O_1)}{\tilde{k}_{de}(s;O_1)} \tag{4.8}$$

It can be shown[10] that the similar equations can also be written for methyl shift and PCP steps. The above equation therefore can be written for the more general case as

$$\frac{\tilde{k}_{isom}(t;s)}{\tilde{k}_{isom}(s;t)} = \frac{\tilde{k}_{pr}(s)}{\tilde{k}_{pr}(t)} \frac{\tilde{k}_{de}(t;O_i)}{\tilde{k}_{de}(s;O_i)} \tag{4.9}$$

or, in terms of equilibrium constants as,

$$\frac{\tilde{k}_{isom}(t;s)}{\tilde{k}_{isom}(s;t)} = \frac{\tilde{K}_{pr/de}^{(O_i \rightleftarrows s)}}{\tilde{K}_{pr/de}^{(O_i \rightleftarrows t)}} \tag{4.10}$$

This is a thermodynamically based equation, expressing the relationship of the single event rate coefficients corresponding to the reverse steps of an isomerization reaction between a secondary and tertiary carbenium ions, in terms of two single event equilibrium constants of protonation/deprotonation in which a particular olefin (preferably the reference olefin) is protonated to produce a secondary and tertiary carbenium ions in two separate elementary steps.

4.1.5 Hydrogenation/Dehydrogenation

If the catalyst has sufficient Pt content, it can be assumed that the hydrogenation/ dehydrogenation steps are in quasi-equilibrium and the rate determining step lies at acid sites of the catalyst.[14] Debrabandere et al.[25] argued that the long chain paraffins will be more active at the acid sites because they can undergo more isomerization and cracking steps at the acid site. This might shift the rate determining step from the acid sites to the metal sites for long chain paraffins. For this study however, hydrogenation / dehydrogenation steps are assumed to be in quasi-equilibrium and the equilibrium constants for the hydrogenation/dehydrogenation of all the possible olefins / paraffins are calculated using Benson's group contribution method.

4.1.6 Parameters for Physical Adsorption

In the three phase hydrocracking, it is assumed that the catalyst surface is covered with the liquid phase and therefore, the gas phase is not coming in direct contact with the

catalyst. Under these conditions, the physical adsorption of alkanes can take place from the liquid phase only. In the liquid phase conditions, the zeolite cavities are completely filled with the carbon chain elements and several alkane molecules can be present in the supercages of the zeolites (particularly for zeolites with larger cavities, like zeolite Y). For zeolites with larger cavities, it is rather improbable that at complete saturation of the adsorbent, the adsorbed molecules are perfectly aligned with the walls of the supercages of the zeolites. This means that only a fraction of each alkane molecule experiences the force field exerted by the zeolite structure. A random coiled distribution, in which only a part of the alkane chain is in contact with different areas of the zeolite surface, is more likely. The adsorption potential of the adsorbed alkane molecules, which is dominated by dispersion forces of alkanes, is governed by the interaction of only that part of the alkane chain which is in contact with the zeolite surface and not by all the carbon groups of the molecule. Therefore, if the alkane molecules of different chain length are present in the liquid phase, it can be expected that their partition coefficients should not differ appreciably with chain length. Denayer et al.[18] conducted experiments for the adsorption of alkane molecules of different chain length in a mobile liquid phase of n-octane and found that the partition coefficients of the alkane molecules are almost the same, irrespective of the length of carbon chain. Based on these experimental evidences, only one physisorption equilibrium coefficient is taken for all the molecules irrespective of the chain length. The simulation results obtained from the model based on this assumption predicted a very high percentage of dibranched and tribranched paraffin in the hydrocracking products as compared to those obtained from the experiments. To decreases the percentage of di- and tri-branched paraffins, it was found necessary to employ different physisorption equilibrium coefficients based on the degree of branching of the molecule. This led to the introduction of four different parameters in the model corresponding to the physisorption of normal, mono-, di-, and tri-branched paraffins.

4.2 Summary of Model Parameters

It has been shown that modeling of hydrocracking of paraffins in liquid phase involves the following parameters:

1) Single-event rate coefficients for PCP	4
2) Single-event rate coefficients for β-scission	6
3) Protonation/deprotonation equilibrium constants	2
4) Langmuir physisorption equilibrium constants	4

If the two protonation/deprotonation equilibrium constants i.e., $\tilde{K}_{pr/de}^{(O_r \rightleftarrows s)}$ and $\tilde{K}_{pr/de}^{(O_r \rightleftarrows t)}$ are introduced as the parameters in the model, equation (4.10) can be used to calculate the single event rate coefficient for PCP(t,s) from the single event rate parameter for PCP(s,t), or vice versa. This reduces the number of single event rate parameters for PCP from 4 to 3. In addition to this, it is found that during the formulation of rate equations for the model, $\tilde{K}_{pr/de}^{(O_r \rightleftarrows s)}$ and $\tilde{K}_{pr/de}^{(O_r \rightleftarrows t)}$ always appear in multiplication with the single event rate parameters for PCP and cracking

$$\tilde{k}^{*}(m_{ik}, w_{il}) = \tilde{k}(m_{ik}, w_{il})\tilde{K}_{pr/de}^{(O_r \rightleftarrows m_{ik})} C_{sat} C_t \tag{4.11}$$

where $\tilde{k}(m_{ik}, w_{il})$ is the single event rate coefficient for isomerization or cracking with *m* and *w* as the type of reactant and product carbenium ions, respectively. Refer section 4.3 for the development of the equation 4.11. This particular form is obtained because of the assumption that the surface concentration of the acid sites covered by carbenium ions is very small and therefore, concentration of the vacant acid site is equal to the total acid site concentration. With this assumption, the two equilibrium constants for protonation/deprotonation can be combined with the appropriate single event rate parameters to define the composite rate parameters for PCP and cracking, that can be calculated from the experimental data. This treatment reduces the total number of

independent parameters in the model from 16 to 13. A brief summary of all these model parameters is given in table 4.1.

4.3 Development of Rate Expressions

Paraffin molecules are physically adsorbed in the cages of the zeolite catalyst. Froment et al.[26] modeled the physisorption process in hydrocracking using several isotherms and found that Langmuir isotherm gives the best fit to the experimental data.

$$P_i^{liq} \rightleftarrows P_i^{ads} \tag{4.12}$$

TABLE 4.1: List of Model Parameters

S. No	Parameter	Description
1.	$\tilde{k}^*_{PCP}(s;s)$	Composite single event rate parameters for protonated cyclo propane (PCP)
2.	$\tilde{k}^*_{PCP}(s;t) = \tilde{k}^*_{PCP}(t;s)$	
3.	$\tilde{k}^*_{PCP}(t;t)$	
4.	$\tilde{k}^*_{Cr}(s;s,no)$	Composite single event rate parameters for β-scission
5.	$\tilde{k}^*_{Cr}(s;s,io)$	
6.	$\tilde{k}^*_{Cr}(s;t,no)$	
7.	$\tilde{k}^*_{Cr}(s;t,io)$	
8.	$\tilde{k}^*_{Cr}(t;s,io)$	
9.	$\tilde{k}^*_{Cr}(t;t,io)$	
10.	$K_{L,np}$	Langmuir physisorption equilibrium constants for normal, mono-branch, di-branch and tri-branch paraffins
11.	$K_{L,mbp}$	
12.	$K_{L,dbp}$	
13.	$K_{L,tbp}$	

Assuming that physical adsorption is in quasi-equilibrium, the concentration of the adsorbed paraffins can be given in terms of the measurable paraffin concentrations using the Langmuir isotherm as,

$$C_{P_i}^{ads} = \frac{C_{sat} K_{L_{Pi}} C_{P_i}^{liq}}{1 + \sum_i K_{L_{Pi}} C_{P_i}^{liq}} \tag{4.13}$$

These adsorbed paraffins are dehydrogenated at the metal sites of the catalyst. A particular paraffinic molecule P_i can produce several olefins O_{ij} on dehydrogenation at the metal site of the catalyst, i.e.,

$$P_i^{ads} \rightleftarrows O_{ij}^{liq} + H_2^{liq} \tag{4.14}$$

Here it is assumed that olefins and hydrogen remains in the liquid phase and hydrogenation /dehydrogenation steps are at quasi-equilibrium. This assumption allows calculating the equilibrium concentration of olefins in terms of the concentration of the adsorbed paraffins.

$$C_{O_{ij}}^{liq} = \frac{K_{DH}^{(P_i \rightleftarrows O_{ij})} C_{P_i}^{ads}}{C_{H_2}^{liq}} \tag{4.15}$$

Combining equations (4.13) and (4.15) gives,

$$C_{O_{ij}}^{liq} = \frac{K_{DH}^{(P_i \rightleftarrows O_{ij})} C_{sat} K_{L_{Pi}} C_{P_i}^{liq}}{C_{H_2}^{liq} (1 + \sum_i K_{L_{Pi}} C_{P_i}^{liq})} \tag{4.16}$$

The olefins produced at the metal site are protonated at the acid sites to give the carbenium ions.

$$O_{ij}^{liq} + H^+ \rightleftarrows R_{ik}^+ \tag{4.17}$$

It should be noted that one particular olefin can produce a maximum of two carbenium ions, depending upon the location of the double bond. If the double bond is in the terminal position, one of the produced carbenium ion will be primary and will not be considered in the reaction network. The index *k* in equation (4.17) is used to describe all the possible carbenium ions that can be produced by protonation of all the olefins obtained from P_i on dehydrogenation. As discussed above, protonation/deprotonation steps are in quasi-equilibrium giving the concentrations of the carbenium ions in terms of the olefin concentrations as follows:

$$C_{R_{ik}^+} = K_{pr/de}^{(O_{ij} \rightleftarrows R_{ik}^+)} C_{O_{ij}}^{liq} C_{H^+} \tag{4.18}$$

If there are *n* olefins in equilibrium with a single carbenium ion R_{ik}^+, *n* equations can be written similar to equation (4.18), each describing the equilibrium of R_{ik}^+ with a different olefin. The average concentration of R_{ik}^+ can therefore be given as,

$$C_{R_{ik}^+} = \frac{1}{n} \sum_{j=1}^{n} K_{pr/de}^{(O_{ij} \rightleftarrows R_{ik}^+)} C_{O_{ij}}^{liq} C_{H^+} \tag{4.19}$$

The number *n* will be 2 in case of a secondary carbenium ion and 3 in case of a tertiary carbenium ion. Substituting the concentration of olefins in equation (4.19) from equation (4.16) gives the concentration of the carbenium ions in terms of the liquid phase concentration of paraffins,

$$C_{R_{ik}^+} = \frac{1}{n} \sum_{j=1}^{n} \frac{K_{pr/de}^{(O_{ij} \rightleftarrows R_{ik}^+)} K_{DH}^{(P_i \rightleftarrows O_{ij})} C_{sat} C_{H^+} K_{L_{Pi}} C_{P_i}^{liq}}{C_{H_2}^{liq} (1 + \sum_i K_{L_{Pi}} C_{P_i}^{liq})} \tag{4.20}$$

The (de)protonation and (de)hydrogenation equilibrium constants can now be expressed in terms of the respective single event equilibrium constants, using the following two equations:

$$K_{pr/de}^{(O_{ij} \rightleftarrows R_{ik}^{+})} = \frac{\sigma_{O_{ij}}^{gl}}{\sigma_{R_{ik}^{+}}^{gl}} \tilde{K}_{pr/de}^{(O_{ij} \rightleftarrows R_{ik}^{+})} \tag{4.21}$$

$$K_{DH}^{(P_i \rightleftarrows O_{ij})} = \frac{\sigma_{P_i}^{gl}}{\sigma_{O_{ij}}^{gl} \sigma_{H_2}^{gl}} \tilde{K}_{DH}^{(P_i \rightleftarrows O_{ij})} \tag{4.22}$$

Substituting equations (4.21) and (4.22) in equation (4.20) gives,

$$C_{R_{ik}^{+}} = \frac{1}{n} \left(\frac{\sigma_{P_i}^{gl}}{\sigma_{R_{ik}^{+}}^{gl} \sigma_{H_2}^{gl}} \right) \sum_{j=1}^{n} \frac{\tilde{K}_{pr/de}^{(O_{ij} \rightleftarrows R_{ik}^{+})} \tilde{K}_{DH}^{(P_i \rightleftarrows O_{ij})} C_{sat} C_{H^{+}} K_{L_{Pi}} C_{P_i}^{liq}}{C_{H_2}^{liq} (1 + \sum_{i} K_{L_{Pi}} C_{P_i}^{liq})} \tag{4.23}$$

By using equation (4.24), the single event protonation/deprotonation equilibrium constant $\tilde{K}_{pr/de}^{(O_{ij} \rightleftarrows R_{ik}^{+})}$ can be expressed in terms of the single event protonation / deprotonation equilibrium constant of R_{ik}^{+} with reference olefin, i.e., $\tilde{K}_{pr/de}^{(O_r \rightleftarrows R_{ik}^{+})}$, as discussed in the section 4.1.3.

$$\tilde{K}_{pr/de}^{(O_{ij} \rightleftarrows R_{ik}^{+})} = \tilde{K}_{pr/de}^{(O_r \rightleftarrows m_{ik})} \tilde{K}_{isom}^{(O_{ij} \rightleftarrows O_r)} \tag{4.24}$$

where m_{ik} can be secondary or tertiary depending on the type of carbenium ion R_{ik}^{+}. Substituting equation (4.24) in (4.23) gives the concentration of the carbenium ions as per equation (4.25). This concentration can be used in equation (4.26) to get the rate of consumption of the carbenium ion through an elementary step in which a product carbenium ion R_{il}^{+} of type w (s or t) is formed.

$$C_{R_{ik}^+} = \frac{1}{n}\left(\frac{\sigma_{P_i}^{gl}}{\sigma_{R_{ik}^+}^{gl}\sigma_{H_2}^{gl}}\right)\frac{\tilde{K}_{pr/de}^{(O_r \rightleftarrows m_{ik})} C_{sat} C_{H^+} K_{L_{Pi}} C_{P_i}^{liq}}{C_{H_2}^{liq}(1+\sum_i K_{L_{Pi}} C_{P_i}^{liq})} \sum_{j=1}^{n} \tilde{K}_{isom}^{(O_{ij} \rightleftarrows O_r)} \tilde{K}_{DH}^{(P_i \rightleftarrows O_{ij})} \tag{4.25}$$

$$r_{R_{ik}^+} = n_e \tilde{k}(m_{ik}, w_{il}) C_{R_{ik}^+} \tag{4.26}$$

Equations (4.25) and (4.26) can be combined to give the rate of consumption of carbenium ions as,

$$r_{R_{ik}^+} = n_e \tilde{k}(m_{ik}, w_{il}) \frac{1}{n}\left(\frac{\sigma_{P_i}^{gl}}{\sigma_{R_{ik}^+}^{gl}\sigma_{H_2}^{gl}}\right)\frac{\tilde{K}_{pr/de}^{(O_r \rightleftarrows m_{ik})} C_{sat} C_{H^+} K_{L_{Pi}} C_{P_i}^{liq}}{C_{H_2}^{liq}(1+\sum_i K_{L_{Pi}} C_{P_i}^{liq})} \sum_{j=1}^{n} \tilde{K}_{isom}^{(O_{ij} \rightleftarrows O_r)} \tilde{K}_{DH}^{(P_i \rightleftarrows O_{ij})} \tag{4.27}$$

Svoboda et al.[14] showed that the total concentration of active acid sites occupied by carbenium ions at the solid surface is negligible as compared to the total active acid site concentration C_t. Therefore, it can be assumed that the concentration of the vacant active acid sites C_{H^+} can be approximated equal to the total active acid sites concentration C_t in equation (4.27). Further, it can be seen from equation (4.27) that the factor $\tilde{K}_{pr/de}^{(O_r \rightleftarrows m_{ik})} C_{sat} C_{H^+}$ in the numerator is a constant and can be combined with the single event rate coefficient to give a composite single event rate coefficient as,

$$\tilde{k}^*(m_{ik}, w_{il}) = \tilde{k}(m_{ik}, w_{il}) \tilde{K}_{pr/de}^{(O_r \rightleftarrows m_{ik})} C_{sat} C_t \tag{4.28}$$

The resulting equation for the rate of consumption of carbenium ions can now be written as,

$$r_{R_{ik}^+} = n_e \tilde{k}^*(m_{ik}, w_{il}) \frac{1}{n}\left(\frac{\sigma_{P_i}^{gl}}{\sigma_{R_{ik}^+}^{gl}\sigma_{H_2}^{gl}}\right)\frac{K_{L_{Pi}} C_{P_i}^{liq}}{C_{H_2}^{liq}(1+\sum_i K_{L_{Pi}} C_{P_i}^{liq})} \sum_{j=1}^{n} \tilde{K}_{isom}^{(O_{ij} \rightleftarrows O_r)} \tilde{K}_{DH}^{(P_i \rightleftarrows O_{ij})} \tag{4.29}$$

In the above equation, $C_{P_i}^{liq}$ is the liquid phase concentration of a particular paraffinic molecule P_i. In the practical situations, it is not possible to have the composition of the feed at a molecular level because of the limitations of the analytical methods. This can be accounted for by means of a posteriori lumping technique which incorporates the detailed knowledge of the elementary steps from the reaction network. The lumps are defined based on the degree of branching for each carbon number, therefore, four lumps namely n-paraffins, mono-branch paraffins, di-branch paraffins and tri-branch paraffins are used for each carbon number. Here it should be noted that lumps containing n-paraffins will have only one component, and thus they are pure components not lumps. This lumping scheme is therefore called 'partial lumping'. These lumps are judiciously selected based on the criteria that the individual components of a lump rapidly reach the reaction equilibrium as a result of the fast hydride shift and methyl shift steps.[27] This is the condition for rigorous lumping which is satisfied with paraffins. The reaction scheme shown in Figure 4.3 is observed between these lumps for each carbon number.

To implement this reaction scheme, the 'global' rate of conversion of one lump into the other lump has to be calculated. Using equation (4.29), the rate of consumption of a particular lump/pure component L_m through l type of elementary step involving reactant and product carbenium ions of type m and w respectively can be calculated by using the following equation:

$$r_{L_m,l_{m,w}}^{Cons} = \frac{\tilde{k}_l^*(m,w) K_{L,L_m} C_{L_m}^{liq}}{C_{H_2}^{liq}\left(1+\sum_{Nc} K_{L,L_m} C_{L_m}^{liq}\right)} \sum_{q=1}^{q_T} n_{e,q} y_{i,L_m} \frac{1}{n}\left(\frac{\sigma_{P_i}^{gl}}{\sigma_{R_{ik}^+}^{gl}\sigma_{H_2}^{gl}}\right) \sum_{j=1}^{n} \tilde{K}_{isom}^{(O_{ij}\rightleftarrows O_r)} \tilde{K}_{DH}^{(P_i\rightleftarrows O_{ij})} \qquad (4.30)$$

In the above equation y_{i,L_m} is the equilibrium mole fraction of the isomer P_i of lump L_m. The index l can be PCP or cracking and m & n can be either secondary or tertiary. q_T is the total number of $l_{m,w}$ type of elementary steps consuming the components of lump L_m.

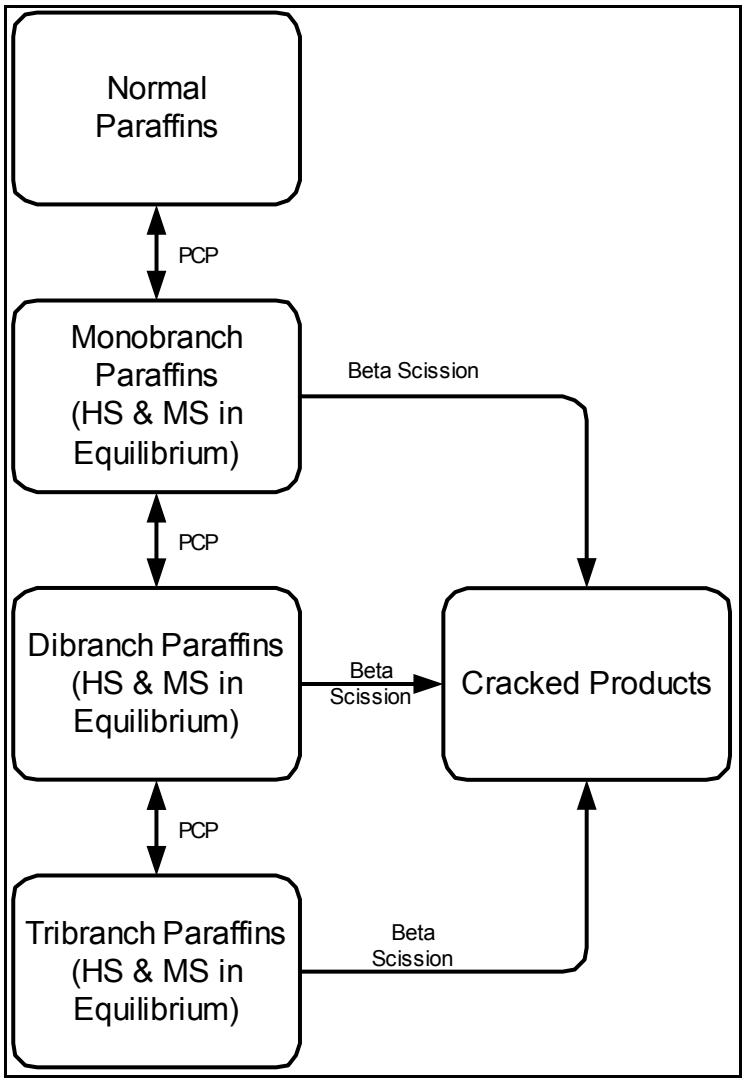

Figure 4.3 Reaction scheme between the lumps/components per carbon number

Equation (4.30) can be simplified into,[24]

$$r_{L_m,l_{m,w}}^{Cons} = LCC_{L_m,l_{m,w}} \frac{\tilde{k}_l^*(m,w) K_{L,L_m} C_{L_m}^{liq}}{C_{H_2}^{liq}(1+\sum_{Nc} K_{L,L_m} C_{L_m}^{liq})} \tag{4.31}$$

$$\text{where } LCC_{L_m,l_{m,w}} = \sum_{q=1}^{q_T} n_{e,q} y_{i,L_m} \frac{1}{n} \left(\frac{\sigma_{P_i}^{gl}}{\sigma_{R_{ik}^+}^{gl} \sigma_{H_2}^{gl}} \right) \sum_{j=1}^{n} \tilde{K}_{isom}^{(O_{ij} \rightleftarrows O_r)} \tilde{K}_{DH}^{(P_i \rightleftarrows O_{ij})} \tag{4.32}$$

$LCC_{L_m,l_{m,w}}$ in the above equations is the lumping coefficient for consumption of the lump L_m through l type of elementary steps involving reactant and product carbenium ions of type m and w respectively.

The corresponding rate of formation of lump L_m from all other lumps can be given by

$$r^{Form}_{L_m,l_{m,w}} = \sum_{k=1}^{Nc} LCF_{L_m,L_k,l_{m,w}} \frac{\tilde{k}_l^{*}(m,w) K_{L,L_k} C^{liq}_{L_k}}{C^{liq}_{H_2}(1+\sum_{Nc} K_{L,L_k} C^{liq}_{L_k})} \tag{4.33}$$

$$\text{where} \quad LCF_{L_m,L_k,l_{m,w}} = \sum_{q=1}^{q_T} n_{e,q} y_{i,L_k} \frac{1}{n} \left(\frac{\sigma^{gl}_{P_i}}{\sigma^{gl}_{R^+_{ik}} \sigma^{gl}_{H_2}} \right) \sum_{j=1}^{n} \tilde{K}^{(O_{ij} \rightleftarrows O_r)}_{isom} \tilde{K}^{(P_i \rightleftarrows O_{ij})}_{DH} \tag{4.34}$$

is lumping coefficients for the formation of lump L_m from lump L_k through l type of elementary steps involving reactant and product carbenium ions of type m and w respectively.

Equations (4.31) and (4.33) now can be used to get the net rate of formation of lump L_m as follows:

$$r^{Net}_{L_m} = \sum_{l=1}^{n_l} (r^{Form}_{L_m,l_{m,w}} - r^{Cons}_{L_m,l_{m,w}}) \tag{4.35}$$

In the above equation, n_l is the number of all the possible types of elementary steps considered in the model.

CHAPTER V

PARAMETER ESTIMATION AND REACTOR SIMULATION RESULTS

5.1 Reactor Model and Parameter Estimation

Experimental data for the hydrocracking of n-hexadecane on a specific catalyst have been collected in a bench scale tubular reactor operated under isothermal conditions at three different temperatures.

At the given conditions the reactor operates in trickle flow regime with a fixed bed of porous catalyst particles, a vapor phase and a liquid phase flowing cocurrently. In a trickle flow regime, a continuous gas phase exists with a dispersed liquid phase flowing as a laminar film or rivulets over the catalyst particles.[28] To estimate the parameters from the experimental data, a one dimensional isothermal reactor model has been formulated in which both liquid and gas phases are considered in plug flow. For n-hexadecane hydrocracking, a total of 49 lumps and pure components including hydrogen are required. The model consists of continuity equations for hydrogen, the components and lumps in the gas and liquid phase requiring a total of 98 continuity equations. It is assumed that the gas and liquid are perfectly distributed and that all the particles are completely wet. With this assumption, the continuity equations for the gas phase will only account for the mass transfer between the gas and liquid phases. The interphase mass transfer flux is described in terms of the two film model[28]

$$N_i = k_{o,i}, \left(\frac{C_i^G}{H_i} - C_i^L \right) \tag{5.1}$$

$$with \frac{1}{k_{o,i}} = \frac{1}{k_G H_i} + \frac{1}{k_L} \tag{5.2}$$

The interphase mass transfer flux is calculated for each component/lump and the continuity equations for the gas phase components are formulated as follows,

$$\frac{1}{\Omega}\frac{dF_i^G}{dz} = -k_{o,i}a_v\left[\frac{C_i^G}{H_i} - C_i^L\right] \quad i = 1, 2.....N_C \tag{5.3}$$

The continuity equations for liquid phase components also take into account the net rate of formation of component/lump *i,*

$$\frac{1}{\Omega}\frac{dF_i^L}{dz} = \left(k_{o,i}a_v\left[\frac{C_i^G}{H_i} - C_i^L\right] + r_i\right) \quad i = 1, 2.....N_C \tag{5.4}$$

The set of ordinary differential equations defined by equations (5.3) and (5.4) is solved for the initial boundary conditions given by the feed composition as,

$$F_i^G = F_i^{G,o} \; and \; F_i^L = F_i^{L,o} \; at \; z = 0, \quad i = 1, 2.....N_C$$

The value of the liquid phase mass transfer coefficient $k_L a_v$ has been calculated from a correlation given by Sato[29] and the gas side mass transfer coefficient $k_G a_v$ is calculated from Reiss'[30] correlation. The gas-liquid interfacial area a_v is calculated by the correlation given by Charpentier.[31] The values of the Henry coefficients are calculated using the Peng-Robinson equation of state.

The integration of the system of ODEs along the axial direction of reactor is carried out using Adam's predictor-corrector method. The molar flow rates of component/lump *i* in the gas phase and in the liquid phase obtained from the continuity equations are added to get the total molar flow rate of component/lump *i.* The total molar flow rate of component/lump *i* thus obtained is converted into the percent molar flow rate based on

total hydrocarbons at the reactor exit (on a hydrogen free basis) and are finally used as responses in the parameter estimation. The i^{th} response calculated from the model is given as,

$$\hat{y}_i = \frac{F_i^G + F_i^L}{\sum_{j=1}^{N_C-1}\left(F_j^G + F_j^L\right)} \times 100 \tag{5.5}$$

The index N_C represents H_2 and it is excluded from the summation in the above equation. The estimation of the model parameters has been performed by minimization of the weighted residual sum of squares of the responses for all the observations at one temperature, i.e.,

$$\Re(\beta) = \sum_{i=1}^{nresp}\sum_{j=1}^{nobs} w_i\left[y_{i,j} - \hat{y}_{i,j}(\beta)\right]^2 \tag{5.6}$$

In equation (5.6) β is the set of model parameters, $y_{i,j}$ is the experimental value of the i^{th} response of the j^{th} observation and $\hat{y}_{i,j}$ the corresponding value calculated using the model. Weighting factors w_j are the diagonal elements of the inverse of the covariance matrix of the experimental errors of the responses determined from the replicate experiments. However, in the absence of replicate experiments, appropriate weighting factors depending on the importance and relative numerical values of responses has been used to get the best overall fit of the experimental data to the model. Because of high non-linearity of the objective function, it has been found that a constrained optimization algorithm is necessary for the estimation of parameters. Non-negativity of rate coefficients and physisorption equilibrium constants sets the lower bound of all the parameters to zero. Appropriate upper bounds for the parameters have been set based on the nature of the parameters. A constrained sequential quadratic algorithm has been used to estimate the model parameters.[32]

5.2 Sensitivity Study of Parameters

The model parameters are estimated separately at three different temperatures. The parameter values are provided in Table 5.1.

TABLE 5.1: Parameters Estimated from Experimental Data

	Temperature (^oC)	299.0	321.3	332.4	Correlation Coefficient, R^2
	Composite Single-event Rate Coefficients				
1	$\tilde{k}^*_{PCP}(s;s)$	18.493	31.631	49.325	0.9778
2	$\tilde{k}^*_{PCP}(s;t)$	5,559.982	9,266.636	23,629.923	0.8678
3	$\tilde{k}^*_{PCP}(t;t)$	4,238.080	6,054.400	10,292.480	0.9030
4	$\tilde{k}^*_{Cr}(s;s,no)$	926.203	1,117.832	1,138.209	0.9433
5	$\tilde{k}^*_{Cr}(s;s,io)$	202.013	243.808	248.253	0.9433
6	$\tilde{k}^*_{Cr}(s;t,no)$	1,997.853	2,411.202	2,709.137	0.9952
7	$\tilde{k}^*_{Cr}(s;t,io)$	9,529.041	11,500.566	14,989.072	0.9117
8	$\tilde{k}^*_{Cr}(t;s,io)$	5,267.623	6,357.476	10,357.389	0.8071
9	$\tilde{k}^*_{Cr}(t;t,io)$	11,629.882	14,036.064	14,291.930	0.9433
	Physical Adsorption Equilibrium Constants				
10	$K_{L,np}$	0.041	0.035	0.027	0.8845
11	$K_{L,mbp}$	0.087	0.061	0.045	0.9742
12	$K_{L,dbp}$	1.071	0.765	0.560	0.9671
13	$K_{L,tbp}$	18.480	9.941	8.747	0.9749

It has been found that the model is more sensitive to some of these parameters as compared to others. For example, $\tilde{k}^{*}_{PCP}(s;s)$ and $K_{L,np}$ are the two parameters to which the model is most sensitive. These parameters govern the total conversion and isomerization conversion. This is because the feed to the reactor is n-hexadecane, and therefore, there is always a high concentration of unconverted n-hexadecane through out the reactor. The high concentration of n-hexadecane as compared to the other branched paraffins makes the model more sensitive to the physisorption equilibrium constant for n-paraffins, i.e, $K_{L,np}$, than the other three physisorption parameters. An increase in the value of this parameters drastically increases the adsorbed concentration of n-hexadecane giving rise to a higher rate of conversion of n-hexadecane to the mono-branch hexadecane isomers. Since the β-scission steps can only take place from the branched paraffins, the cracking conversion also increases significantly with the increase in the value of $K_{L,np}$.

The explanation for the model sensitivity to $\tilde{k}^{*}_{PCP}(s;s)$ can be given parallel to that of $K_{L,np}$. Here it should be mentioned that the secondary carbenium ions coming from n-paraffins, or in other words, the linear secondary carbenium ions (i.e., without any side chains) can only be consumed through PCP(s,s). And since, there is a high concentration of n-hexadecane, a correspondingly high concentration of linear secondary carbenium ions exists inside the reactor attributing a higher weight to $\tilde{k}^{*}_{PCP}(s;s)$. An increase in the value of this parameter increases the conversion of n-hexadecane, similar to $K_{L,np}$.

Out of the six rate parameters for β-scission (from 4 to 9 in Table 5.1), the model is more sensitive to the first four, namely, $\tilde{k}^{*}_{Cr}(s;s,no)$, $\tilde{k}^{*}_{Cr}(s;s,io)$, $\tilde{k}^{*}_{Cr}(s;t,no)$ and, $\tilde{k}^{*}_{Cr}(s;t,io)$ than the last two, i.e., $\tilde{k}^{*}_{Cr}(t;s,io)$ and $\tilde{k}^{*}_{Cr}(t;t,io)$. Moreover, the parameter $\tilde{k}^{*}_{Cr}(t;t,io)$ has much less weight than $\tilde{k}^{*}_{Cr}(t;s,io)$. The only possible reason for this behavior is that

there are very few elementary steps in which $\tilde{k}^{*}_{Cr}(t;t,io)$ is involved. It can be seen that to produce a tertiary carbenium ion and an iso-olefin as the product of β- scission from a tertiary carbenium ion, the reactant carbenium ion must have three methyl branches in such a way that the β carbon atom with respect to the positive charge is a quaternary carbon. The example for this type of reactant carbenium is shown in Figure 5.1.

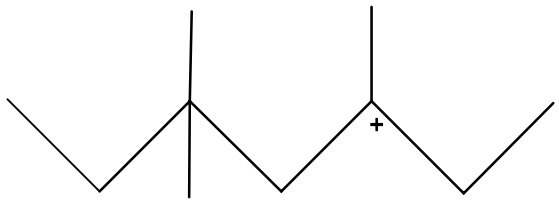

Figure 5.1 Structure of reactant giving a t-carbenium ion and an iso-olefin on cracking

As can be seen from the product profiles [Figures 5.7, 5.11 & 5.15], the concentration of branched hydrocarbons decreases with increasing the degree of branching, i.e., in the case of hydrocracking of n-paraffins, the concentration of n-paraffins is maximum while that of tri-branch paraffins is minimum, with intermediate values of mono- and di-branched paraffins in decreasing order. Moreover, the concentration of tri-branched paraffins producing the tertiary carbenium ions having the characteristic skeleton structures shown above will be even smaller, attributing a very low weight to the parameter $\tilde{k}^{*}_{Cr}(t;t,io)$. Similar reasoning can be given to explain the low weight of the parameter $\tilde{k}^{*}_{Cr}(t;s,io)$. However, since $\tilde{k}^{*}_{Cr}(t;s,io)$ can take place from a di-branched carbenium ion also, there can be more elementary steps involving this parameters as compared to $\tilde{k}^{*}_{Cr}(t;t,io)$ making the model more sensitive to it than the latter.

As discussed above, the differences in sensitivity of the model for different parameters can be explained primarily based on difference in the concentration of carbenium ions to which the respective parameters are associated. Therefore, it can be argued that the

sensitivity of the model for various parameters can be quite different if the hydrocracking of a highly branched paraffinic feed is carried out in place of the hydrocracking of n-paraffins. On the same line of thought, it is expected that the differences in the sensitivity of model for various parameters will vanish if hydrocracking feed is a mixture of paraffins having different degrees of branching. In other words, for such a feed the model will be almost equally sensitive to all the parameters and therefore, parameter estimation from such a feed should provide better and more significant values of the parameters.

5.3 Temperature Dependency of the Parameters

As shown in section 4.3, the composite single event rate parameters for isomerization and cracking can be given by the following expression

$$\tilde{k}_i^*(m,w) = C_t C_{sat} \tilde{K}_{pr/de}^{(O_r \rightleftarrows m)} \tilde{k}_i(m,w) \tag{5.7}$$

The single event rate coefficient and the protonation/deprotonation equilibrium constant can be written as functions of temperature by using Arrhenius law and vant Hoff's law, respectively.

$$\tilde{k}_i = \tilde{A}_i \exp(-E_i / RT) \tag{5.8}$$

$$\tilde{K}_{pr/de}^{(O_r \rightleftarrows m)} = \tilde{A}_{pr/de} \exp(-\Delta H_{pr/de}^{(O_r \rightleftarrows m)} / RT) \tag{5.9}$$

Equations (5.8) and (5.9) can be substituted in equation (5.7) to give the temperature dependency of the composite rate parameters as follows

$$\tilde{k}_i^* = C_t C_{sat} \tilde{A}_i \tilde{A}_{pr/de} \exp\left[\frac{-(\Delta H_{pr/de} + E_i)}{RT}\right] \tag{5.10}$$

It should be noted that the value of activation energy E_i will be positive whereas the energy of protonation step, $\Delta H_{pr/de}$ will be negative. This is because the energy of the protonated olefin, i.e., the carbenium ion is lass than the corresponding olefin making the protonation step exothermic in nature. Equation (5.10) can also be written as

$$\ln \tilde{k}_i^* = \ln(C_t C_{sat} \tilde{A}_i \tilde{A}_{pr/de}) - \left[\frac{(\Delta H_{pr/de} + E_i)}{R}\right]\frac{1}{T} \tag{5.11}$$

showing that the plot of $\ln \tilde{k}_i^*$ vs. $\frac{1}{T}$ will give a straight line facilitating the calculation of composite single event rate parameters at any desired temperature. Similarly, the last four parameters representing the physisorption equilibrium constants can also be written as the function of temperature using vant Hoff's equation. The variation of different parameters with temperatures is plotted in Figures 5.2 to 5.5 and the corresponding correlation coefficients obtained by linear regressions are given in Table-5.1.

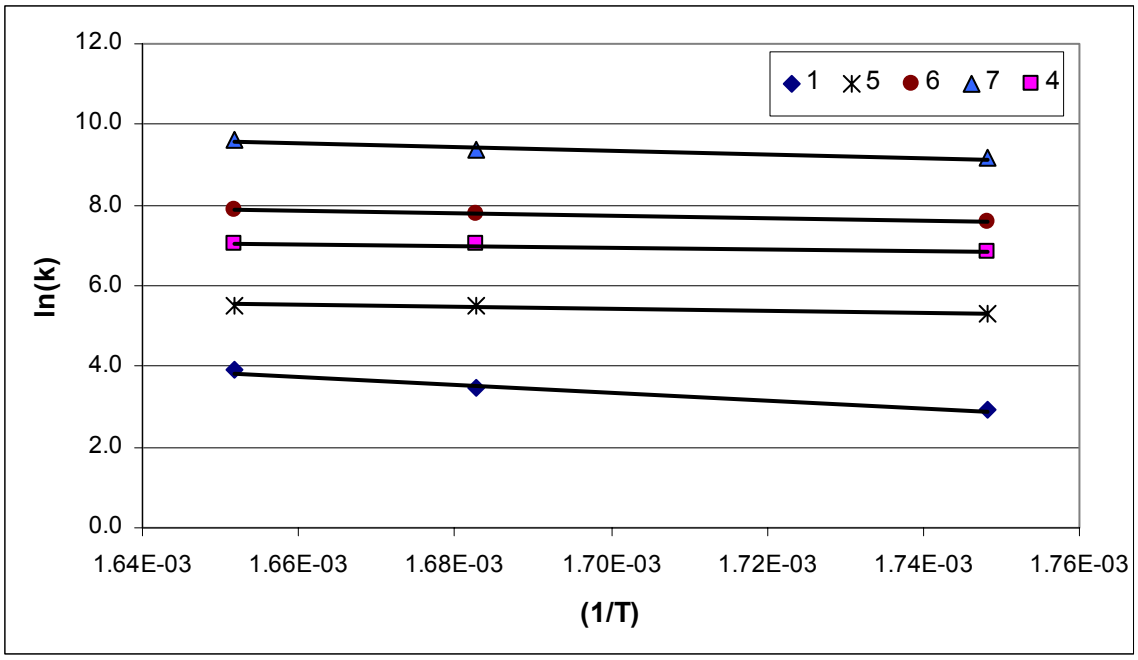

Figure 5.2 Temperature dependency of parameters

$1\text{-}\tilde{k}^*_{PCP}(s;s)$, $4\text{-}\tilde{k}^*_{Cr}(s;s,no)$, $5\text{-}\tilde{k}^*_{Cr}(s;s,io)$, $6\text{-}\tilde{k}^*_{Cr}(s;t,no)$, $7\text{-}\tilde{k}^*_{Cr}(s;t,io)$

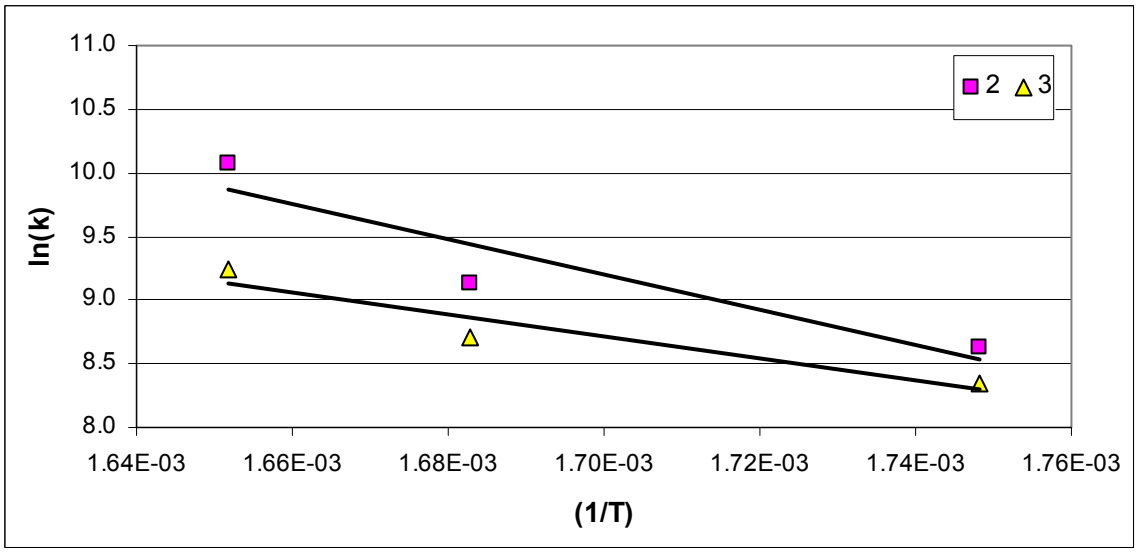

Figure 5.3 Temperature dependency of parameters

$2\text{-}\tilde{k}^*_{PCP}(s;t)$, $3\text{-}\tilde{k}^*_{PCP}(t;t)$

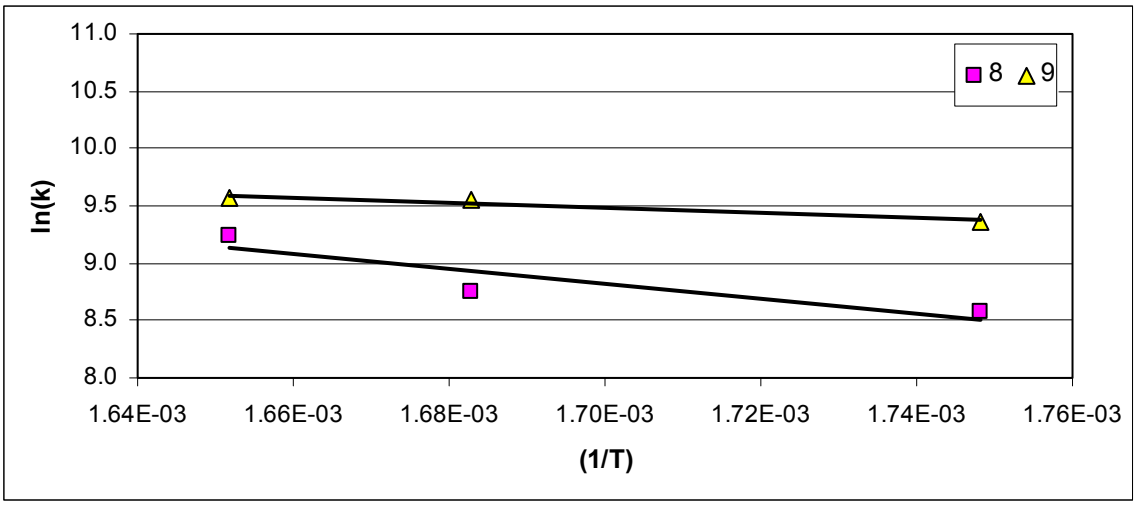

Figure 5.4 Temperature dependency of parameters

8- $\tilde{k}^{*}_{Cr}(t;s,io)$, 9- $\tilde{k}^{*}_{Cr}(t;t,io)$

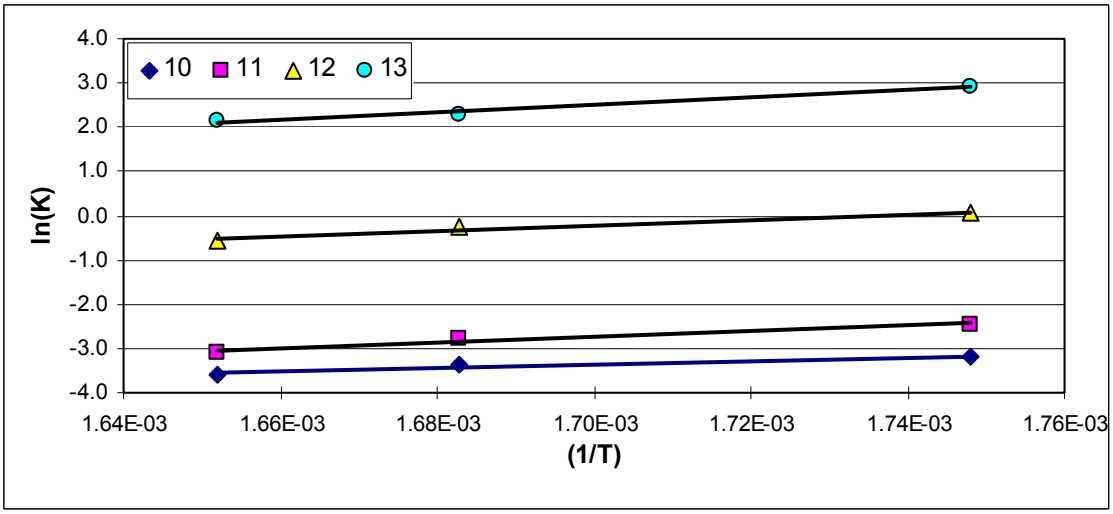

Figure 5.5 Temperature dependency of parameters

10- $K_{L,np}$, 11- $K_{L,mbp}$, 12- $K_{L,dbp}$, 13- $K_{L,tbp}$

5.4 Reactor Simulation Results and Discussion

The optimized parameters are used to study the effect of different process variables on the conversion, product yields and, selectivities. It should be mentioned here that the model parameters are obtained for a given catalyst, and therefore, the effect of changes in the catalyst type or composition can not be studied with these parameters. The effect of temperature, total pressure and the hydrogen to hydrocarbon ratio on the feed conversion and product distribution is discussed in this section. The model is also used to predict the product distribution of hydrocracking of a mixture of heavy paraffins.

5.4.1 Effect of Temperature

Figure 5.6 to 5.9 are the simulated results of hydrocracking of n-hexadecane at a temperature of 304.4 ^{o}C, total pressure of 35.5 bars and hydrogen to hydrocarbon molar ratio (γ) of 9.0. To study the effect of temperature, reactor simulations have been carried out at two other temperatures namely, 321.3 ^{o}C and 332.4 ^{o}C with the same values of total pressure and hydrogen to hydrocarbon ratio. The results at these temperatures are shown in Figures 5.10 to 5.17.

It can be seen from Figures 5.6, 5.10 and 5.14 that the total conversion of n-hexadecane increases with space time at all the temperatures. At a particular value of space time, there is drastic increase in the total conversion with the increase in temperature, and therefore, reactor temperature is one of the most important process parameters to control the feed conversion. Conversion of n- hexadecane to its isomers increases with space time initially and then decreases after passing through a maximum value. The reason for the decrease in isomerization conversion is that initially the reactor is fed with pure n-hexadecane and therefore only linear secondary carbenium ions are formed. These linear secondary carbenium ions can only react through PCP isomerization to produce mono-branch carbenium ions. This can also be seen from Figure 5.18 that at all the temperatures up to approximately 15 % total conversion, isomerization conversion is equal to the total conversion, i.e., all the n-hexadecane is converted to its isomers and no

cracking of isomers takes place. When sufficient concentration of isomers is reached, cracking reactions start taking place. More and more cracking reactions take place as the concentration of isomers increases causing a drop in the moles of hexadecane isomers.

Figures 5.8, 5.12 & 5.16 have the molar distribution of the cracked products based on carbon number at different cracking conversions. The ordinate indicates the moles of products formed per 100 moles of hexadecane cracked. It should be mentioned that if there is no secondary cracking involved, every hexadecane mole will produce two moles of products on cracking. And therefore, irrespective of the cracking conversion, the total moles of cracked products per 100 moles of hexadecane cracked will always be 200. However, Figures 5.9, 5.13 & 5.17 show that the total moles of cracked products formed per 100 moles of hexadecane cracked increases with the cracking conversion. This indicates that as the cracking conversion increases, more and more secondary cracking takes place. In the secondary cracking reactions, products obtained from the cracking of hexadecane are further cracked to produce lighter products. This behavior is evident from Figures 5.8, 5.12 & 5.16, showing that as the cracking conversion increases, the moles of heavier products decreased while those of lighter products increased. The effect of temperature on the extent of secondary cracking can be investigated from Figure 5.19 in which molar product distribution has been plotted at different temperatures at a constant value of cracking conversion. It can be seen that almost the same distribution of cracked products, and therefore, the same number of total cracked products are obtained irrespective of the temperature. Therefore as long as the total pressure and γ are kept constant, product selectivities are only a function of cracking conversion.

5.4.2 Effect of Total Pressure

Simulations have been carried out at different values of the reactor total pressure at a temperature of 304.4 ^{o}C and H_2/HC molar ratio, $\gamma = 9.0$. It can be seen from Figure 5.20 that the total hexadecane conversion and cracking conversion decreases as the reactor pressure is increased, whereas the isomerization conversion increases with pressure. The

reason for this behavior is that at a high pressure, the solubility of hydrogen and therefore, the concentration of hydrogen in the liquid phase increases. It should be noticed that for paraffinic feeds, the order of reaction with respect to hydrogen is negative. This can be seen from equations (4.29) and (4.30) that liquid phase hydrogen concentration appears in the denominator of the rate equation and therefore the increase in the total pressure decreases the rate of reactions reducing the conversion. It should be noted that the above discussion and the dependency of conversion on total pressure is valid only for paraffinic feeds and for 'ideal' hydrocracking taking place in a three phase reactor. In ideal hydrocracking it is assumed that hydrogenation/dehydrogenation reactions are very fast and reach equilibrium so that the rate determining steps are on the acid sites of the catalyst. This assumption may not be always valid, especially for catalyst having a weak metal function. It has also been studied by Debrabandere et al.[25] that rate determining step will tend to shift from acid sites to the metal sites as the chain length of the paraffinic feed is increased. It can also be expected that if the total pressure is reduced below a certain level, the hydrogen concentration in the liquid phase may drop below the equilibrium hydrogen concentration at that temperature. Under all these circumstances, the above assumption of ideal hydrocracking will not be valid and the conversion of the feed may have a different trend with the change in pressure.

In most practical situations, the hydrocracking feedstocks are not pure n-paraffins, rather, they are complex hydrocarbon mixtures like VGO. These feedstocks contain a large amount of aromatics which can only be cracked after their hydrogenation to naphthenes. Aromatics causes deactivation of the catalyst because of the formation of polynuclear aromatics (PNAs) which act as coke precursors. A high hydrogen concentration in such cases increases the rate of hydrogenation of aromatics and also cleans up the catalyst by hydrogenating PNA to increase the life cycle of the catalyst. Moreover, at high hydrogen concentrations, the denitrification of organic nitrogen compounds is also increased. These nitrogenous compounds are highly detrimental to the catalyst activity. These positive effects of high pressure offsets the disadvantage of

low conversion and therefore industrial hydrocracking processes are carried out at higher pressures.

5.4.3 Effect of Hydrogen to Hydrocarbon Ratio

In the three phase hydrocracking, changing the hydrogen to hydrocarbon ratio does not make any appreciable change in the conversion and product distribution. This is because the concentration of hydrogen in the liquid phase is responsible for hydrogenation/dehydrogenation of paraffins. At a constant temperature and total pressure, concentration of hydrogen in the liquid phase is constant and therefore, changing the hydrogen to hydrocarbon ratio over small range does not change the conversion and product distribution significantly. However, as this ratio is increased, vaporization of hydrocarbons increases, and after a certain value, all the hydrocarbons may vaporize switching the three phase hydrocracking to vapor phase hydrocracking. In contrast to the three phase hydrocracking, hydrogen to hydrocarbon ratio has a very pronounced effect on the conversion in gas phase hydrocracking. This is because in gas phase at constant temperature and pressure, increasing the hydrogen to hydrocarbon ratio increases the partial pressure of hydrogen. Since hydrogen partial pressure will appear in the denominator of the rate equations (4.29) and (4.30), conversion of feed will decreases significantly with the increase in the H_2/HC ratio.

The concentration profiles of hydrogen in the gas phase and in the liquid phase along the reactor are plotted in Figures 5.22 and 5.23, respectively.

5.4.4 Reactor Simulation for a Different Feed

The parameters obtained from n-hexadecane hydrocracking are used for reactor simulation to obtain the product distribution for a heavy paraffinic feedstock having normal paraffins from C_9 to C_{33}. A total of 117 lumps/pure components are required for this feed. The detailed composition of the feed and products obtained from the model is given in Table 5.2 and the feed and product composition per carbon number are

compared in Figure 5.24. The simulation is carried out at a temperature of 304.3 ^{o}C, total pressure of 35.5 bars, hydrogen to hydrocarbon molar ratio of 35.5, and liquid hourly space velocity of 1 hr^{-1}. The evolution of different commercial products obtained from hydrocracking namely, LPG, gasoline, middle distillates (MSD) and residuals along the bed length are plotted in Figure 5.25.

TABLE 5.2: Feed and Product Composition for the Heavy Paraffinic Mixture

C-No	Normal Paraffins (Mole %)		Iso Paraffins (Mole %)		Total Paraffins (Mole %)	
	Feed	Product	Feed	Product	Feed	Product
3	0.00	1.27	0.00	0.00	0.00	1.27
4	0.00	0.92	0.00	3.50	0.00	4.42
5	0.00	2.72	0.00	4.14	0.00	6.86
6	0.00	2.43	0.00	4.29	0.00	6.72
7	0.00	2.19	0.00	4.40	0.00	6.59
8	0.00	1.94	0.00	4.52	0.00	6.46
9	0.18	1.81	0.00	4.61	0.18	6.43
10	0.41	1.70	0.00	4.68	0.41	6.38
11	0.45	1.53	0.00	4.69	0.45	6.23
12	0.44	1.32	0.00	4.67	0.44	5.99
13	0.00	0.96	0.00	4.55	0.00	5.51
14	0.39	0.93	0.00	4.43	0.39	5.36
15	0.00	0.64	0.00	4.14	0.00	4.78
16	0.30	0.58	0.00	3.81	0.30	4.39
17	0.00	0.38	0.00	3.32	0.00	3.70
18	0.45	0.34	0.00	2.88	0.45	3.22
19	1.23	0.33	0.00	2.49	1.23	2.83
20	1.92	0.26	0.00	2.04	1.92	2.30
21	2.57	0.21	0.00	1.61	2.57	1.82
22	3.79	0.16	0.00	1.28	3.79	1.44
23	6.29	0.18	0.00	1.18	6.29	1.36
24	10.52	0.18	0.00	1.24	10.52	1.42
25	12.88	0.18	0.00	1.21	12.88	1.39
26	13.39	0.12	0.00	1.01	13.39	1.14
27	12.17	0.09	0.00	0.79	12.17	0.88
28	10.46	0.04	0.00	0.53	10.46	0.57
29	8.17	0.02	0.00	0.31	8.17	0.33
30	6.20	0.00	0.00	0.15	6.20	0.15
31	3.91	0.00	0.00	0.05	3.91	0.05
32	2.39	0.00	0.00	0.01	2.39	0.01
33	1.48	0.00	0.00	0.00	1.48	0.00
Total	100.00	23.46	0.00	76.54	100.00	100.00

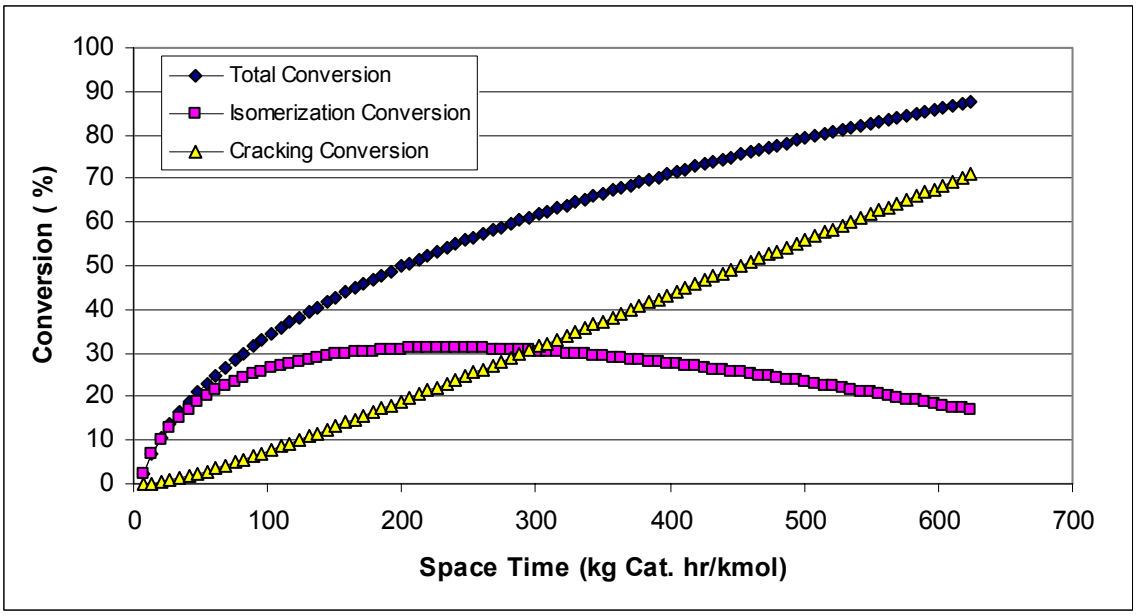

Figure 5.6 Conversion of hexadecane with space time (P = 35.5 bars, T = 304.4 ^{o}C & γ = 9.0)

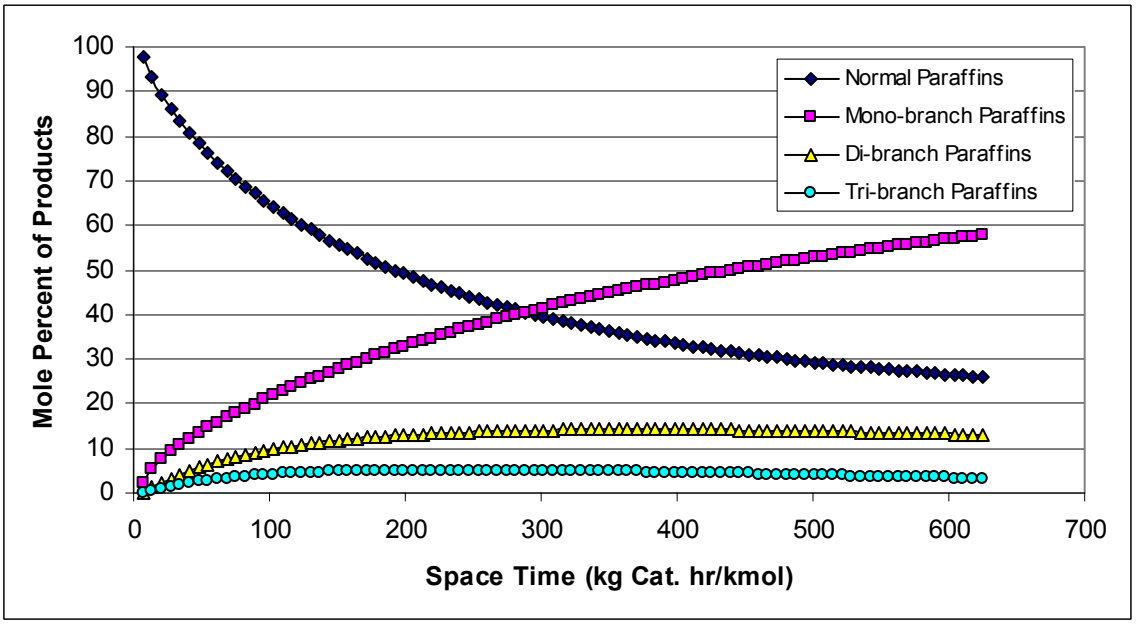

Figure 5.7 Molar distribution of products based on degree of branching (P = 35.5 bars, T = 304.4 ^{o}C & γ = 9.0)

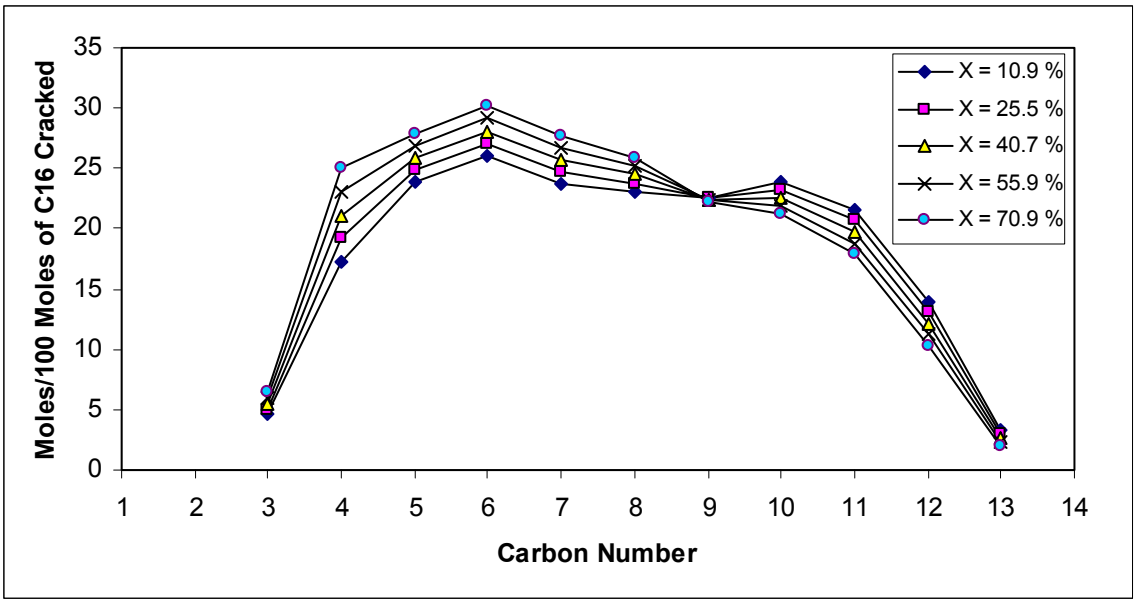

Figure 5.8 Selectivities of products based on carbon number at different cracking conversions (P = 35.5 bars, T = 304.4 ^{o}C & γ = 9.0)

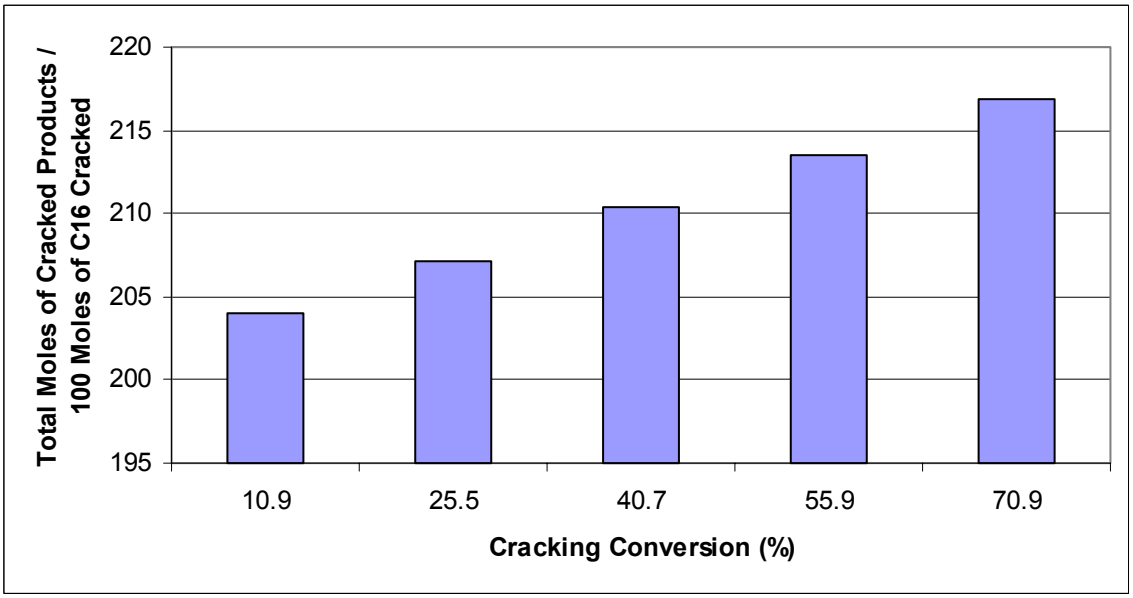

Figure 5.9 Total moles of cracked products formed per 100 moles of hexadecane cracked at different cracking conversions (P = 35.5 bars, T = 304.4 ^{o}C & γ = 9.0)

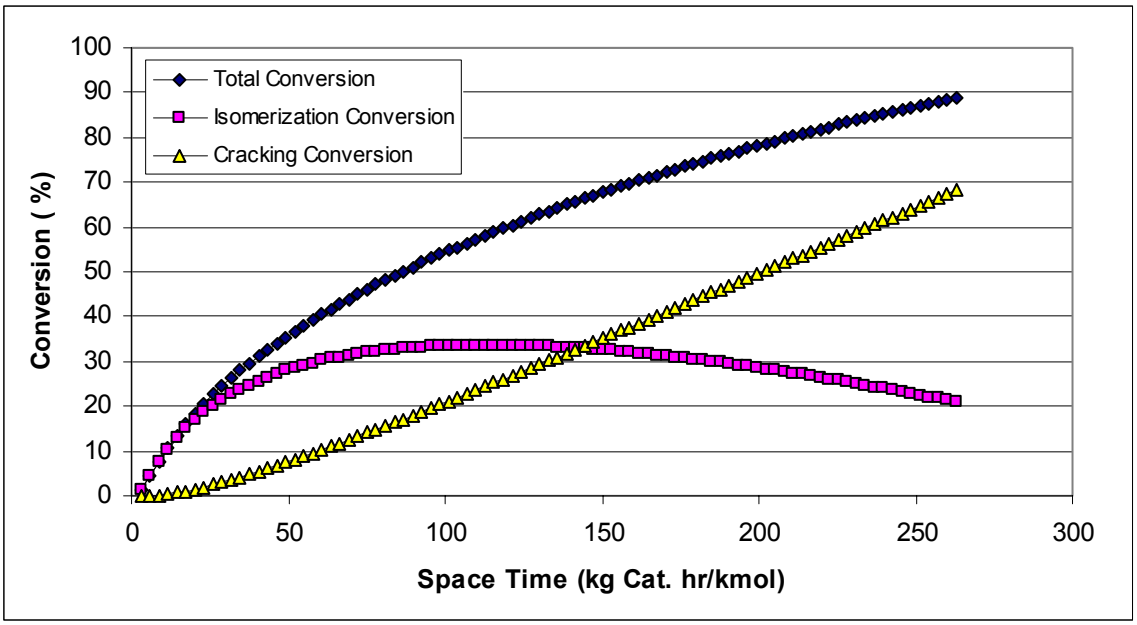

Figure 5.10 Conversion of hexadecane with space time (P = 35.5 bars, T = 321.3 ^{o}C & γ = 9.0)

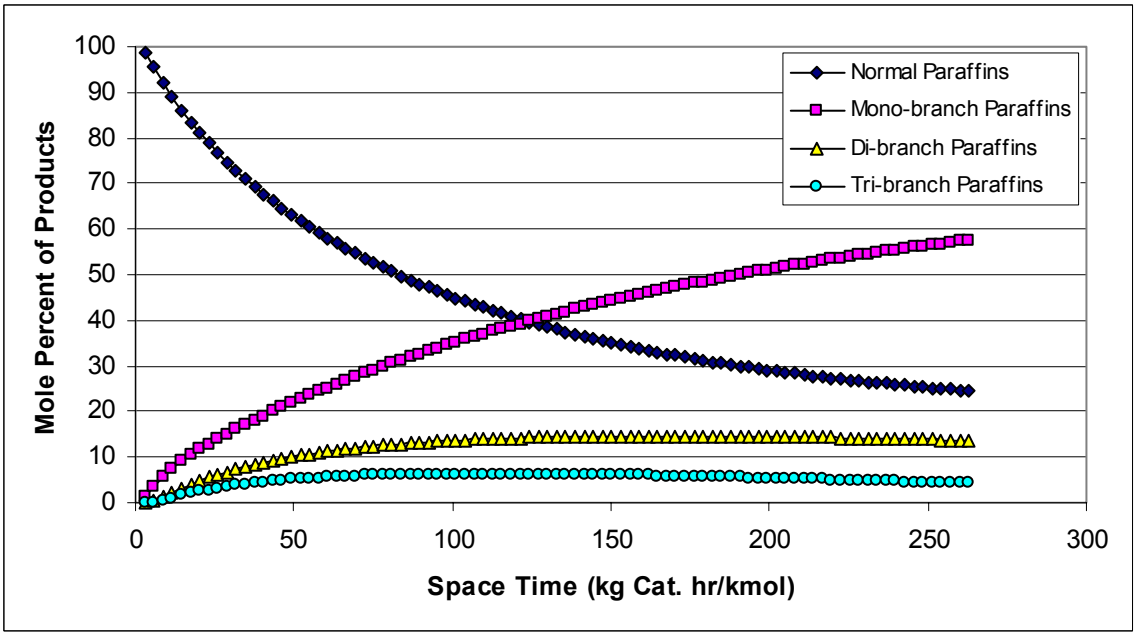

Figure 5.11 Molar distribution of products based on degree of branching (P = 35.5 bars, T = 321.3 ^{o}C & γ = 9.0)

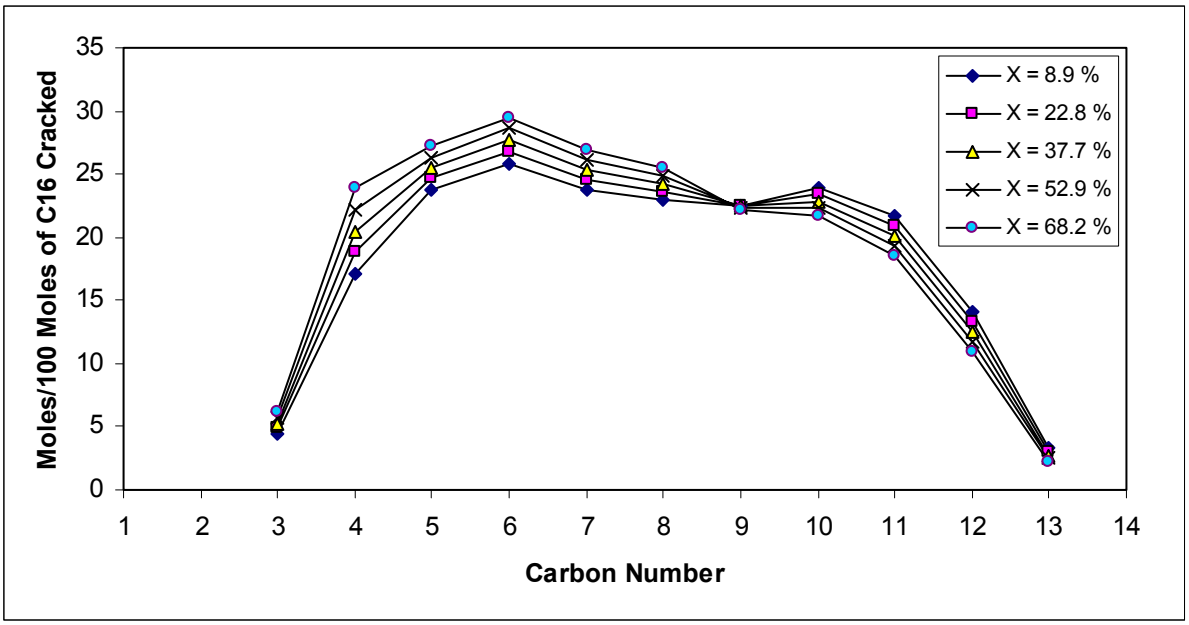

Figure 5.12 Selectivities of products based on carbon number at different cracking conversions (P = 35.5 bars, T = 321.3 ^{o}C & γ = 9.0)

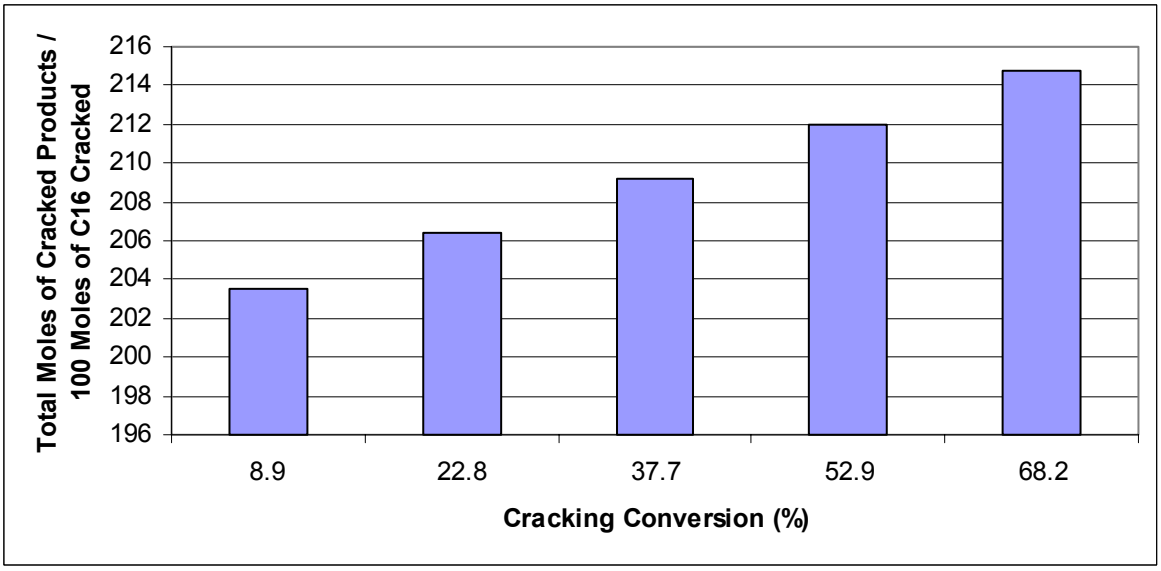

Figure 5.13 Total moles of cracked products formed per 100 moles of hexadecane cracked at different cracking conversions (P = 35.5 bars, T = 321.3 ^{o}C & γ = 9.0)

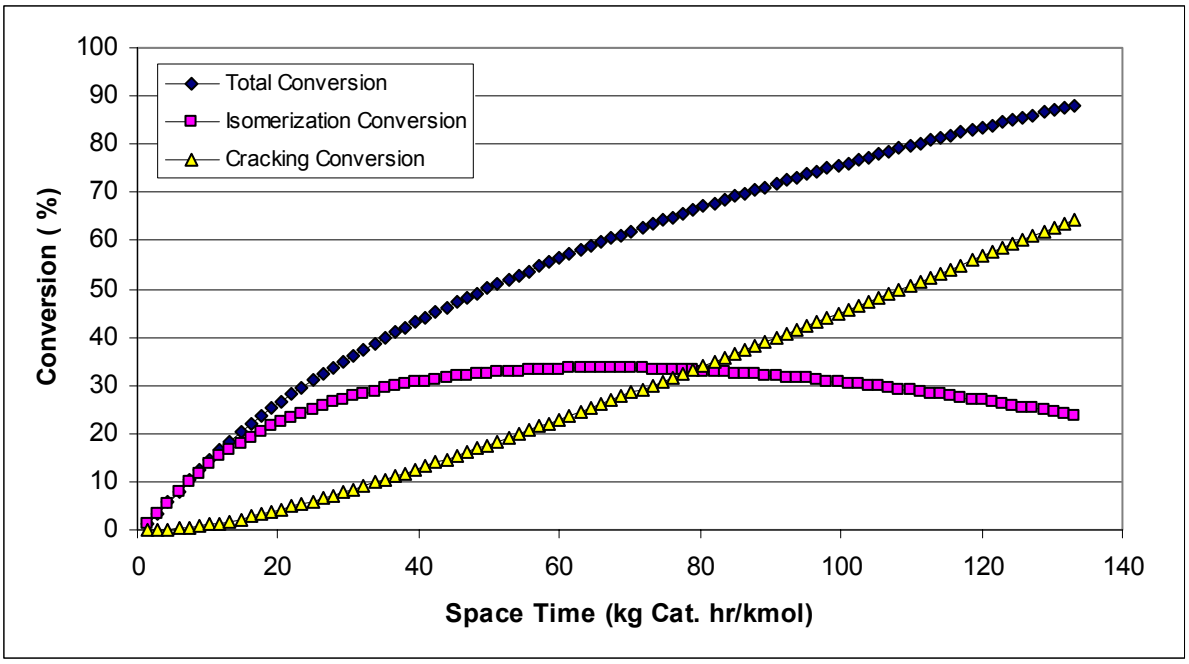

Figure 5.14 Conversion of hexadecane with space time (P = 35.5 bars, T = 332.4 ^{o}C & γ = 9.0)

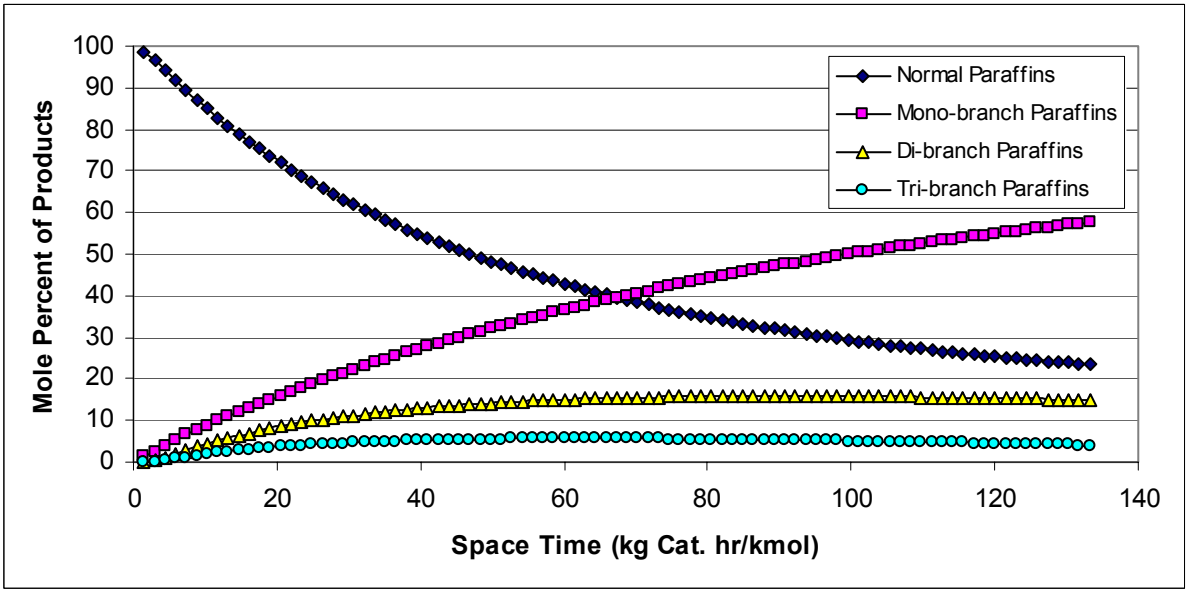

Figure 5.15 Molar distribution of products based on degree of branching (P = 35.5 bars, T = 332.4 ^{o}C & γ = 9.0)

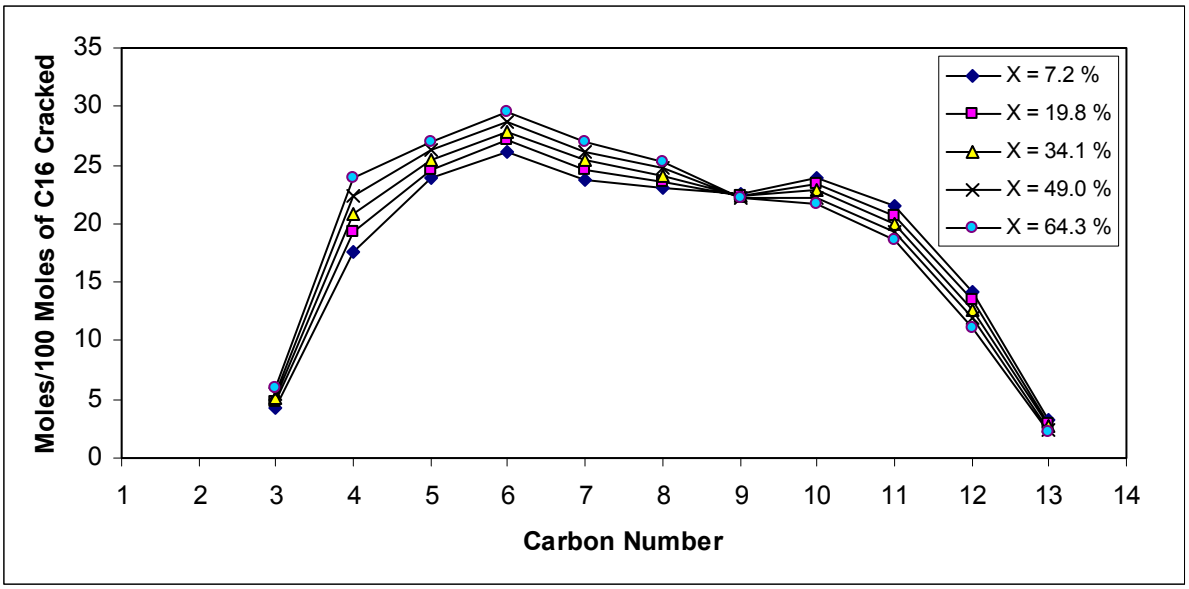

Figure 5.16 Selectivities of products based on carbon number at different cracking conversions (P = 35.5 bars, T = 332.4 ^{o}C & γ = 9.0)

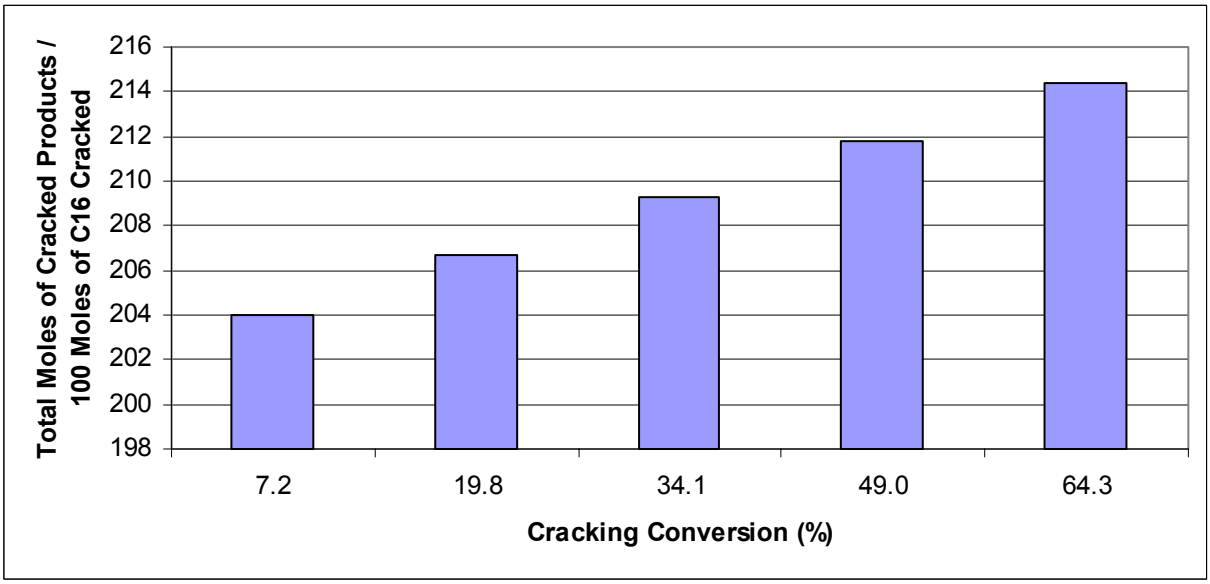

Figure 5.17 Total moles of cracked products formed per 100 moles of hexadecane cracked at different cracking conversions (P = 35.5 bars, T = 332.4 ^{o}C & γ = 9.0)

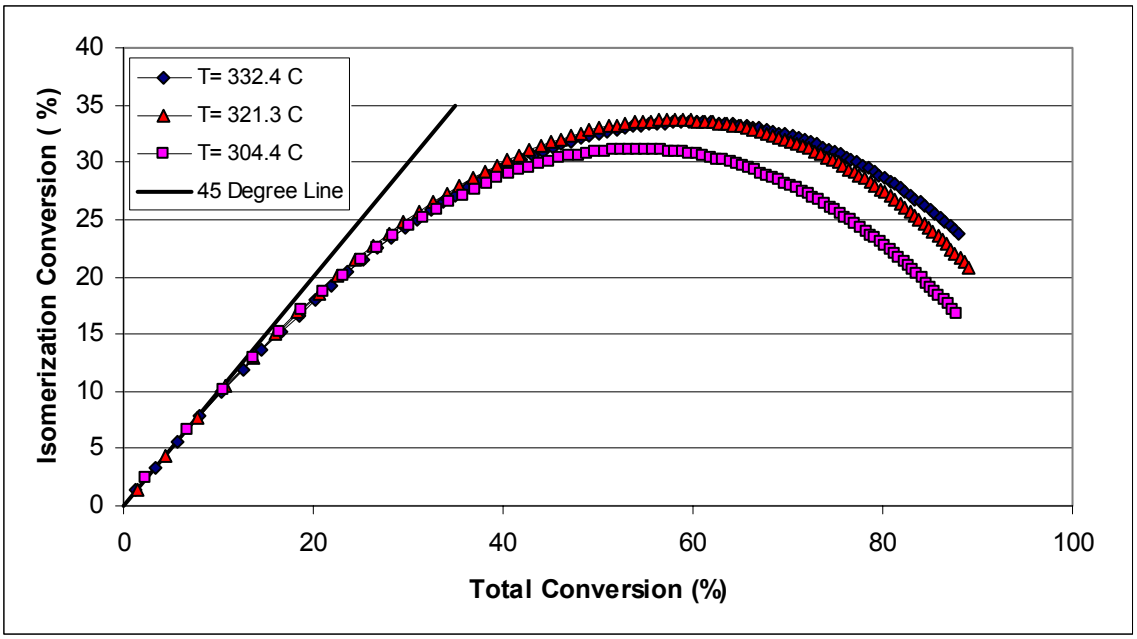

Figure 5.18 Isomerization conversion vs. total conversion at different temperatures (P = 35.5 bars & γ = 9.0)

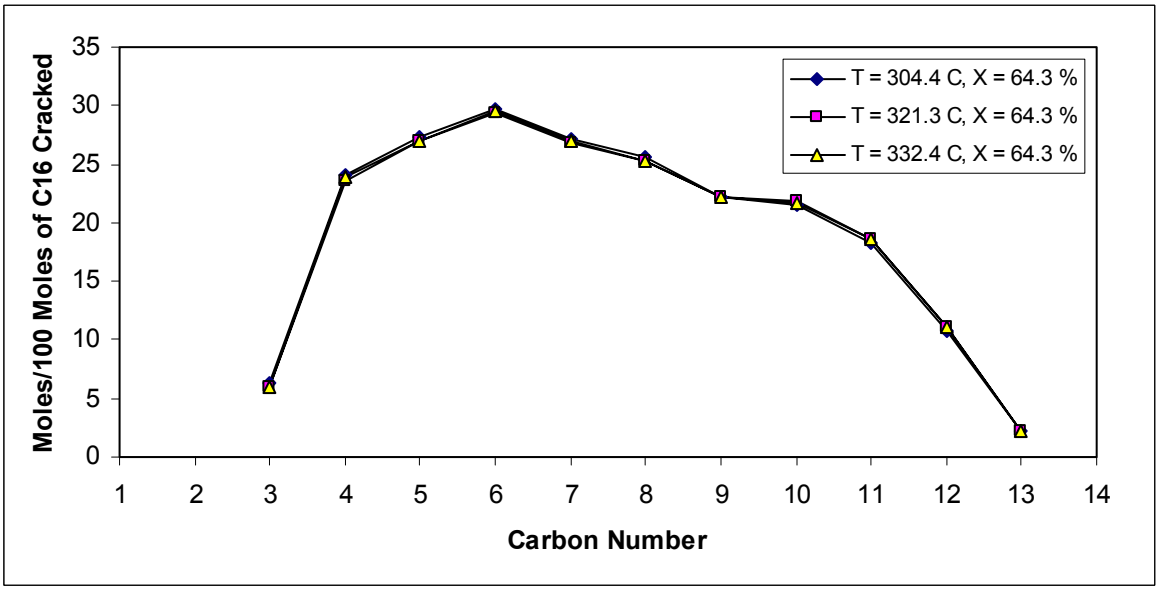

Figure 5.19 Selectivities of products based on carbon number at different temperatures and same cracking conversion (P = 35.5 bars & γ = 9.0)

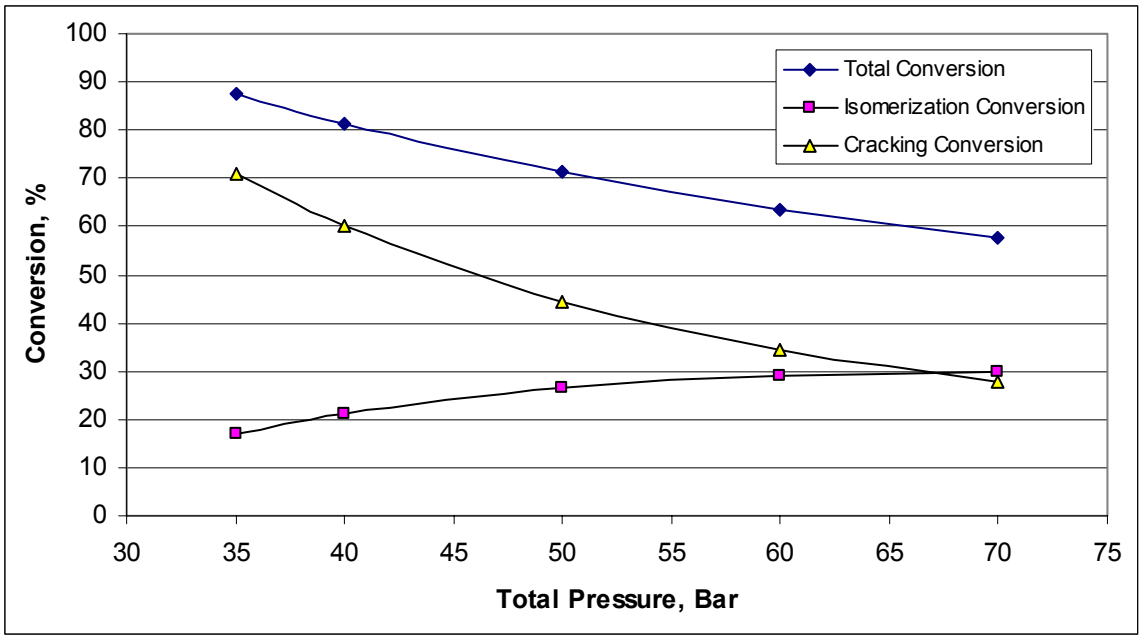

Figure 5.20 Effect of total pressure at the hexadecane conversion (T = 304.4 ^{o}C, γ = 9.0)

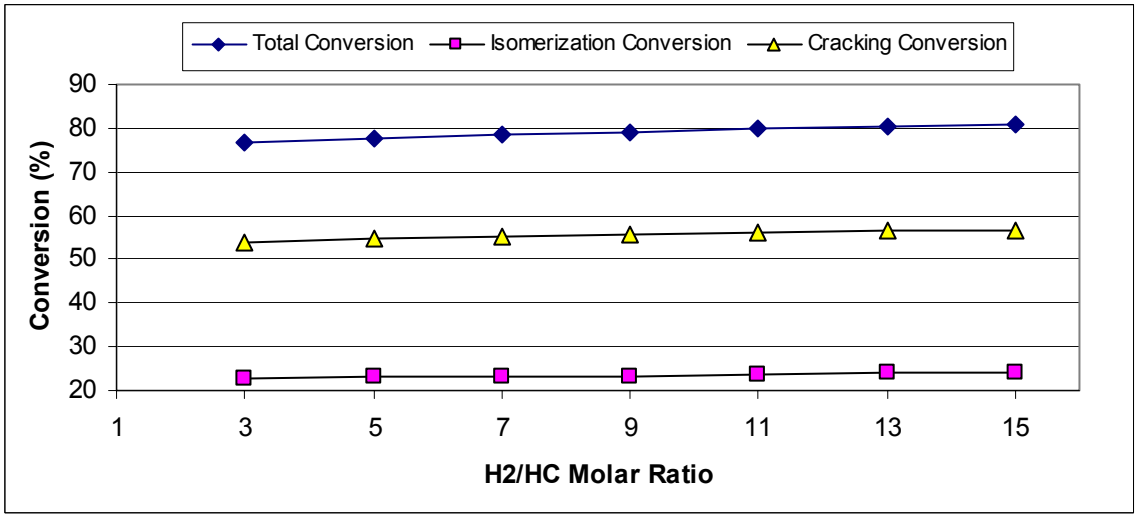

Figure 5.21 Effect of hydrogen to hydrocarbon ratio on conversion (T = 304.4 ^{o}C, P = 35.5 bar, space time = 500.0 kg cat. h/kmol)

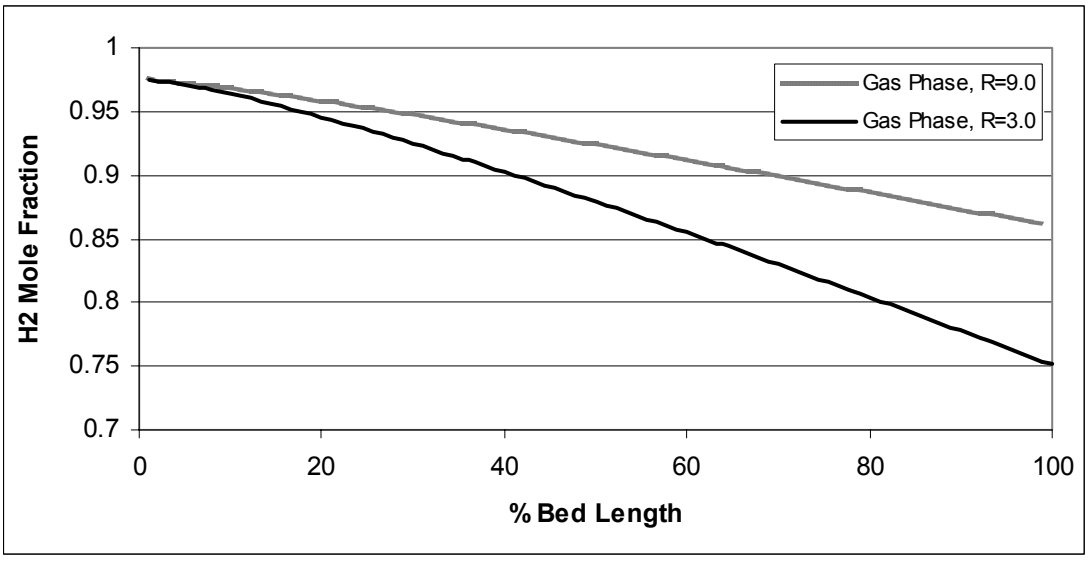

Figure 5.22 Concentration profile of hydrogen in gas phase along the bed length at different values of H_2 to HC ratio R (T = 304.4 ^oC, P = 35.5 bar)

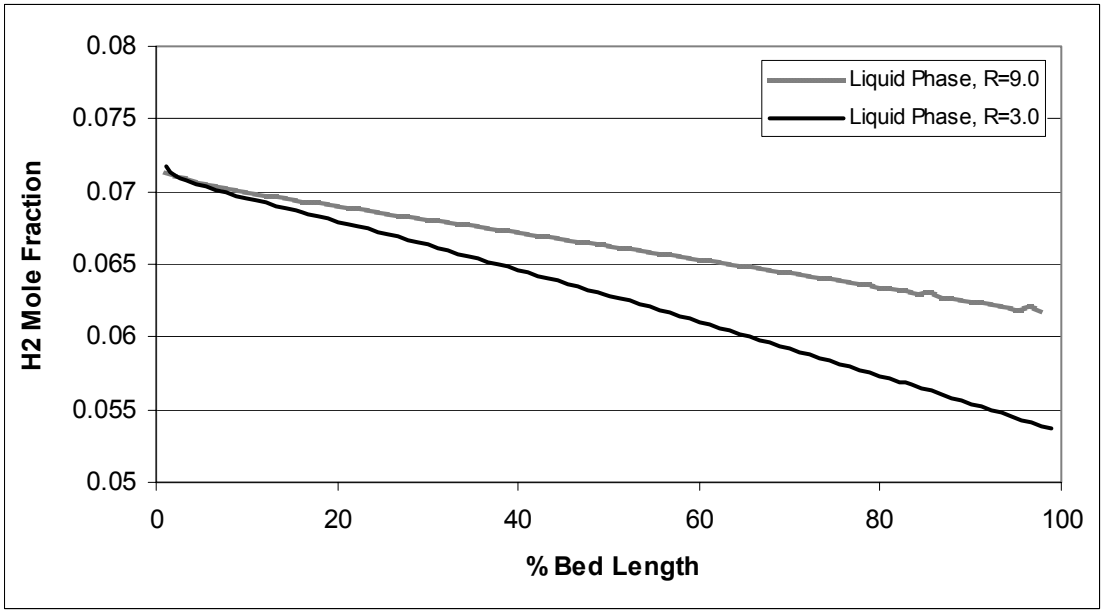

Figure 5.23 Concentration profile of hydrogen in liquid phase along the bed length at different values of H_2 to HC ratio R (T = 304.4 ^oC, P = 35.5 bar)

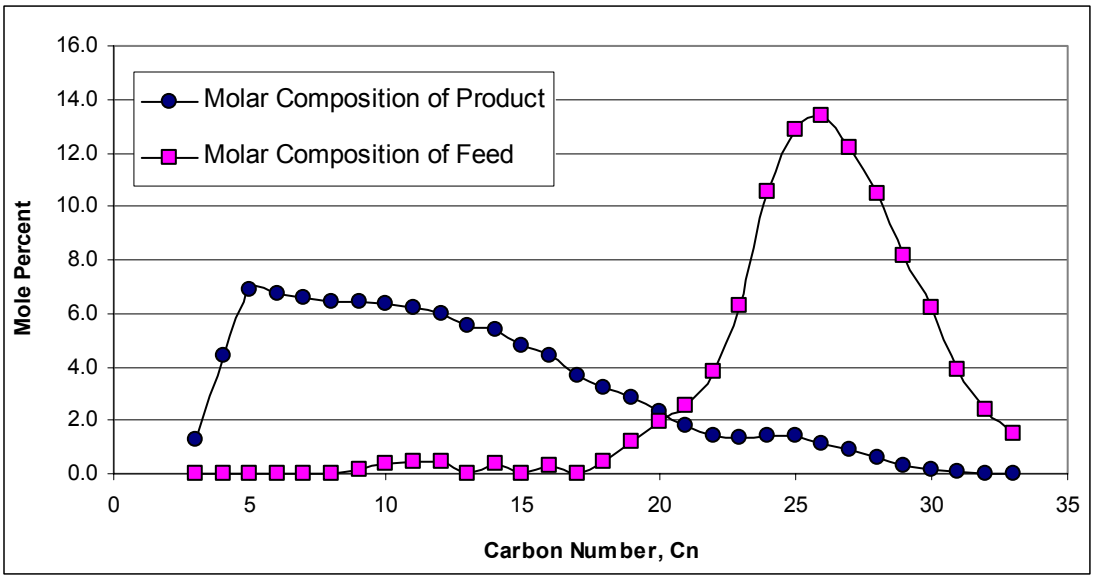

Figure 5.24 Product distribution per carbon number for the heavy paraffinic feed (T = 321.3 ^{o}C, P = 35.5 bar, γ = 35.5, LHSV = 1.0 hr^{-1})

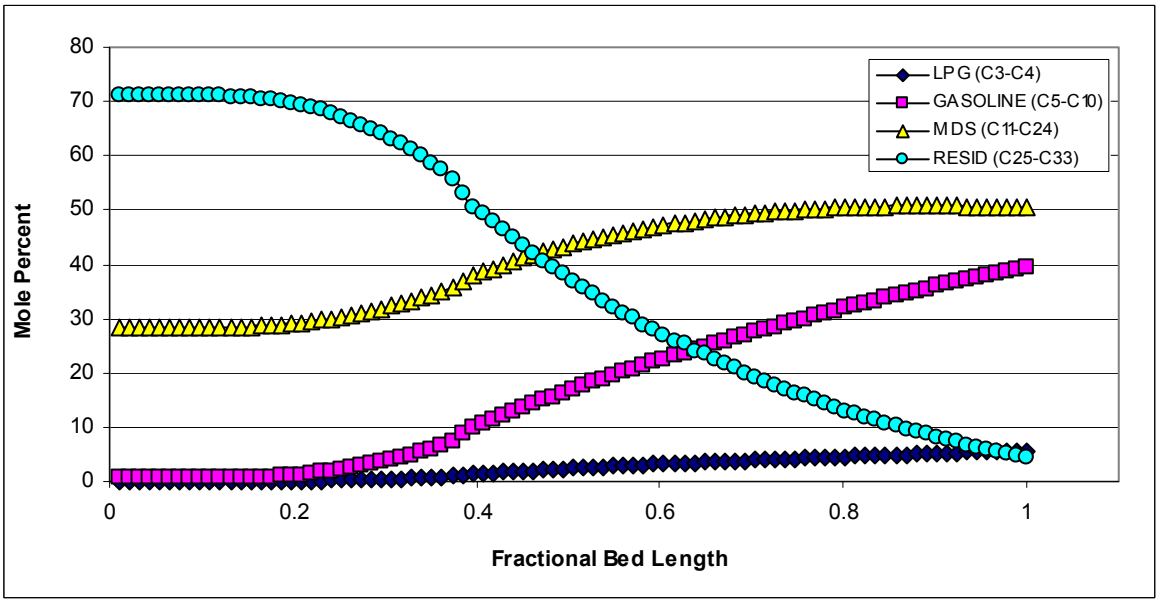

Figure 5.25 Product profiles along the bed length for the heavy paraffinic feed (T = 321.3 ^{o}C, P = 35.5 bar, γ = 35.5, LHSV = 1.0 hr^{-1})

CHAPTER VI

SUMMARY AND CONCLUSIONS

A mechanistic kinetic model for hydrocracking of paraffins based on single event approach has been studied. The model parameters are estimated at three different temperatures. As a result of the fundamental nature of the model, the parameters are only the function of temperature for a specific type of catalyst. The temperature dependency of the single event rate parameters and physisorption parameters has been explained by Arrhenius and vant Hoff's laws respectively facilitating the estimation of the parameters at any desired temperature. As the model parameters are invariant with respect to the feed composition, product profiles for different paraffinic feedstocks can be studied without any further fitting of the model for other feedstocks.

The optimized parameters are used to simulate the reactor at different operating conditions to analyze their effect on the feed conversion and product distribution. It has been shown that the total conversion and cracking conversion increases with space time whereas the isomerization conversion first increases and then decreases. Feed conversion is a strong function of temperature and increases rapidly as the later is increased. It is shown however, that distribution of cracked products is a unique function of cracking conversion irrespective of the reaction temperature. Unlike temperature, conversion decreases with the increase in the pressure because of an increase in the hydrogen concentration in the liquid phase at higher pressures. However, if the rate determining step shifts from acid sites to metal sites, the conversion is expected to have a more complex behavior with pressure. Hydrogen to hydrocarbon ratio on the other hand does make any appreciable change in the conversion. The model is also used to predict the products distribution from the hydrocracking of a heavy paraffinic feed.

NOMENCLATURE

a_v	Gas-liquid interfacial area per unit reactor volume, m_i^2/m_r^3
C_i^G	Molar concentration of *i* in gas bulk, kmol/m_G^3
C_i^L	Molar concentration of *i* in liquid bulk, kmol/m_L^3
$C_{L_m}^{liq}$	Liquid phase concentration of lump L_m, kmol/m_L^3
C_{sat}	Saturation surface concentration of physisorbed hydrocarbons, kmol/ kg of catalyst
C_{H^+}	Surface concentration of vacant acid sites, kmol/ kg of catalyst
C_t	Total surface concentration of acid sites, kmol/ kg of catalyst
$C_{L_m}^{liq}$	Concentration of lump L_m in liquid phase, kmol/ m_r^3
F_i^G	Molar flow rate of *i* in gas phase, kmol/hr
F_i^L	Molar flow rate of *i* in liquid phase, kmol/hr
h	Planck's constant, kJ.hr/molecule
H_i	Henry's law coefficient of *i*
$\Delta H^{o\ddagger}$	Standard entropy of activation, kJ/kmol
k	Rate coefficient of an elementary step, 1/hr
$\tilde{k}$	Single event rate coefficient, 1/hr
$\tilde{k}_{isom}(m,n)$	Single event rate coefficient for the isomerization of *m* type of carbenium ion to *n* type of carbenium ion, 1/hr
$\tilde{k}_{cr}(m;n,no)$	Single event rate coefficient for the cracking of *m* type of carbenium ion to *n* type of carbenium ion and normal olefin, 1/s
k_B	Boltzmann constant, kJ/K molecule
$k_{o,i}$	Overall mass transfer coefficient of *i* in terms of liquid concentration gradient, m_L^3/m_i^2hr

k_G	Mass transfer coefficient from gas bulk to gas-liquid interface, based on concentration driving force, m_G^3/m_i^2hr
k_L	Mass transfer coefficient from gas-liquid interface to liquid bulk, based on concentration driving force, m_L^3/m_i^2hr
K_{L,P_i}	Langmuir physisorption equilibrium constant of paraffin P_i, m_r^3/kmol
K_{L,L_m}	Langmuir physisorption equilibrium constant of lump L_m, m_r^3/kmol
n_e	Number of single events
N_C	Number of components/lumps in the model
N_i	Mass transfer flux of *i* from gas bulk to the liquid bulk, kmol/m_i^2hr
r_i	Net rate of formation of *i*, kmol/m_r^3/hr
R	Gas constant, kJ/kmol K
$\Delta\hat{S}^{o\ddagger}$	Standard entropy of activation, kJ/kmol K
T	Temperature, K
X	Cracking conversion, %
z	Axial coordinate in the reactor, m_r
γ	H_2/HC molar ratio
Ω	Cross-sectional area of reactor, m_r^2
σ_{EXT}	External symmetry number of a species
σ_{INT}	Internal symmetry number of a species
σ_i	Symmetry number of species *i*
σ_{gl}	Global symmetry number of a species

REFERENCES

(1) Scherzer, J.: Gruia, A. J. *Hydrocracking Science and Technology,* Marcel Dekker Inc.: New York, 1996; p 174.

(2) Böhringer, W.; Kotsiopoulos, A.; Fletcher, J. C. *International R&D Forum on Oil, Gas and Petrochemicals,* Kuala Lumpur, Malaysia*,* April 5-6, 2004, 1.

(3) Fox III, J. M. *Catal. Rev.-Sci. Eng.* **1993**, *35*, 169.

(4) Gregor, J. H. *Catal. Lett.* **1990**, *7*, 317.

(5) Govindhakannan, J.; Ph.D. Dissertation, *Modeling of a Hydrogenated Vacuum Gas Oil Hydrocracker*, Lubbock, Texas, **2003**.

(6) Martens, G. G.; Marin, G. B.; Martens, J. A.; Jacob, P. A.; Baron G. V. *J. of Catalysis.* **2000**, *195*, 253.

(7) Weekman, V. W.; Nace, D. M. *AIChE J*. **1970**, *16*, 397.

(8) Jacob, S. M.; Gross, B.; Voltz, S. E.; Weekman, V. W. *AIChE, J.* **1976**, *22*, 701.

(9) Quann, R. J.; Jaffe, S. B. *Ind. Eng. Chem. Res.* **1992**, *31*, 2483.

(10) Baltanas, M. A.; Van Raemdonck, K. K.; Froment, G. F.; Mohedas, S. R. *Ind. Eng. Chem. Res*. **1989**, *28*, 899.

(11) Vynckier, E.; Froment, G. F.; *Kinetic and thermodynamic lumping of multicomponent mixtures*; Elsevier Science Publishers B. V.: Amsterdam, 1991; **p**131.

(12) Clymans, P. J.; Froment, G. F. *Comp. & Chem. Eng.* **1984**, *8(2)*, 137.

(13) Feng, W.; Vynckier, E.; Froment, G. F. *Ind. Eng. Chem. Res*. **1993**, *32*, 2997.

(14) Svoboda, G. D.; Vynckier, E.; Debrabandere, B.; Froment, G. F. *Ind. Eng. Chem. Res.* **1995**, *34*, 3793.

(15) Park, T. P.; Froment, G. F. *Ind. Eng. Chem. Res*. **2001**, *40*, 4172.

(16) Gauw, Franciscus J. M. M. de; Ph.D. Dissertation, *Kinetic Studies of Alkane Hydroisomerization over Solid Acid Catalysts,* Eindhoven, The Netherlands, **2002**.

(17) Denayer, J. F.; Baron, G. V. *Ind. Eng. Chem. Res*. **1997**, *36*, 3242.

(18) Denayer, J. F.; Bouyermaouen, A.; Baron, G. V. *Ind. Eng. Chem. Res.* **1998**, *37*, 3691.

(19) Blomsma, E.; Martens, J. A.; Jacobs, P. A. *J. Catal.* **1996**, *159*, 323.

(20) Saunders, M.; Vogel, P.; Hagen, E. L.; Rosenfeld, J. *Acc. Chem. Res.* **1973**, *6*, 53.

(21) Martens, J. A.; Jacobs, P. A. *J. Catal.* **1990**, *124*, 357.

(22) Martens, J. A.; Jacobs, P. A. Theoretical *Aspects of Heterogeneous Catalysis;* Van Nostrand Reinhold: New York, 1991; p 52.

(23) Steijns, M.; Froment, G. F. *Ind. Eng. Chem. Prod. Res. Dev.* **1981**, *20*(4), 660.

(24) Govindhakannan, J.; Post Doctoral work at Chemical Engineering Department of Texas A & M University, College Station, Texas, **2003**.

(25) Debrabandere, B.; Froment, G. F. *Hydrotreatment and Hydrocracking of Oil Fractions*; Elsevier Science B. V.,**:** Amsterdam, The Netherlands, 1997; **p**379.

(26) Baltanas, M. A.; Vansina, H.; Froment, G. F. *Ind. Eng. Chem. Prod. Res. Dev.* **1983**, *22*, 531.

(27) Schweitzer, J. M.; Galtier, P.; Schweich, D. *Chem. Eng. Sci*. **1999**, *54*, 2441.

(28) Froment, G. F.; Depauw, G. A.; Vanrysselberghe, V. *Ind. Eng. Chem. Res*. **1994**, *33*, 2975.

(29) Sato, Y.; Hirose, H.; Takahashi, F.; Toda, M. *First Pacific Chemical Engineering Congress*, **1972**, 187.

(30) Reiss, L. P. *Ind. Eng. Chem. Pros. Des. Dev.* **1967**, *6*, 486.

(31) Charpentier *Chem. Eng. Journal* **1976**, *11***,** 161.

(32) Gill, P. E.; Murray, W.; Wright, M. H. *A Fortran package for non-linear programming*; Systems Optimization Laboratory: Stanford, California, **1986**.

VITA

Hans Kumar was born in Shamli, India on April 20, 1979. He received a Bachelor of Engineering Degree in Chemical Engineering from the University of Roorkee, India in July 2000. Then he worked as a process engineer at the Process Design and Development Division of Engineers India Limited, New Delhi, India from July 2000 to July 2002. He joined the graduate program at the Department of Chemical Engineering, Texas A&M University in August 2002 and completed his Master of Science in August 2004. He can be contacted through his parents at his permanent address:

Hans Kumar
C/o Kuldeeep Gupta
H.No:108, Kaka Nagar
Shamli - 247776
U. P. (India)